STUDY OF CONTAMINANT BEHAVIOUR IN A VENTILATED ROOM: A CFD MODELING

A DISSERTATION

*Submitted in partial fulfillment of the
requirements for the award of the degree
of*
MASTER OF TECHNOLOGY
in
CHEMICAL ENGINEERING
(with specialization in Industrial Safety and Hazards Management)

By

M. SWAPNA DEVI

DEPARTMENT OF CHEMICAL ENGINEERING
INDIAN INSTITUTE OF TECHNOLOGY ROORKEE
ROORKEE -247 667 (INDIA)
JUNE, 2007

CANDIDATE'S DECLARATION

I hereby declare that the work, which is being presented in the dissertation, entitled, **"STUDY OF CONTAMINANT BEHAVIOUR IN A VENTILATED ROOM: A CFD MODEL ING"** submitted in partial fulfillment of the requirements for the award of degree of **Master of Technology** in Chemical Engineering with specialization in **"INDUSTRIAL SAFETY AND HAZARDS MANAGEMENT"** submitted in the Department of **CHEMICAL ENGINEERING**, Indian Institute of Technology, Roorkee, India, is an authentic record of my own work carried out under the supervision of **Dr. R. BHARGAVA**, and **Dr. KAILAS L. WASEWAR.**

The matter embodied in this dissertation has been submitted by me for the award of any other degree.
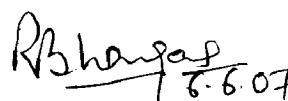
Date:

Place: Roorkee

M. Swapna Devi
(M. SWAPNA DEVI)

CERTIFICATE

This is to certify that above statement made by candidate is correct to best of my knowledge and belief

Dr. Kailas L. Wasewar

Assistant Professor

Department of Chemical Engineering,

Indian Institute of Technology

Roorkee – 247667, INDIA.

Dr. R. Bhargava

Assistant Professor

Department of Chemical Engineering,

Indian Institute of Technology

Roorkee – 247667, INDIA.

ACKNOWLEDGEMENTS

(M. SWAPNA DEVI)

ABSTRACT

One of the most fundamental needs for the mankind is fresh and clean air. It has been estimated that people spend comparatively more time in indoor premises as compared to time spent in outdoor. That created and elevated need for high-quality ventilation systems in buildings. Ventilation is necessary to remove indoor-generated pollutant by diluting these to an acceptable level and to maintain circulation of air by inducing entry of fresh air.

The objective of this thesis is to investigate air flow, contaminant flow and thermal affects in a control panel room connected with a rest room.

To study all aspects as stated above a model is developed and solved using Computation Fluid Dynamics software on a computer.

The commercial Computational Fluid Dynamics (CFD) code PHOENICS, developed by Cham, Version-3.6.1 is used to simulate the model. Laminar and turbulent models are used in simulating the flow in rooms.

Vector and contour plots of velocity, pressure, temperature and contaminant flow are studied. Comparison of laminar model and k-ε model is carried out and found that there are no significant differences between the results of two models under consideration.

CONTENTS

LIST OF FIGURES

LIST OF TABLES

NOMENCLATURE

A	generic property, constant	(-)
C	concentration	(m^3 contaminant /m^3 air)
DR	draught rate	(%)
E	energy	(W)
F	momentum force	(N)
H	specific enthalpy	(J/kg)
P	pressure	(Pa)
Q	airflow rate	(m^3/s)
RT	turbulent reynolds number	(-)
S_h	source term in energy equation	(W/m^3)
T_u	turbulence intensity	(%)
U, V, W	Velocity components in x, y, and z-directions	(m/s)
U_i, U_j, U_k	Tensor notation for velocity components	(m/s)
U_i, V_i, W_i	Tensor notation for mean velocity components	(m/s)
V	volume	(m^3)
g_i, g_j, g_k	Tensor notation for gravitational acceleration	(-)
h_j	enthalpy of species j	(kJ/kg)
Jj	diffusion flux of species j	(kg/m^2s)
k	turbulent kinetic energy	(J/kg)
l_k	Kolmogorov length scale	(m)
$\dot{m}$	mass flow rate of contaminants	(kg/s)
m	mass of contaminants	(kg)
N	number	(particles, cells etc., nd)
p	pressure	(N/m^2 or Pa)
t	Time	(s)
u', v', w'	Velocity fluctuations in x, y, and z-directions	(m/s)
v	velocity	(m/s)
y	distance from the wall	(m)

Greek symbols

ε	rate of dissipation of turbulent kinetic energy	(J/kg s)
ε_c	contaminant removal efficiency	(-)
ε_T	heat removal efficiency	(-)
μ	dynamic viscosity	(kg/ms)
ρ	density	(kg/m^3)
λ	thermal conductivity/specific heat at constant pressure	(-)
σ	molecular Prandtl number	(-)
τ	shear stress	(-)

Empirical non-dimensional constants for k-ε turbulence model

C_μ	0.09
$C_{1\varepsilon}$	depends on flow type
$C_{2\varepsilon}$	depends on flow type
σ_k	depends on flow type
σ_ε	depends on flow type

1.1 INDOOR AIR QUALITY

1.1.1 Indoor air quality concerns

All of us face a variety of risks to our health as we go about our day-to-day lives. Driving in cars, flying in planes, engaging in recreational activities, and being exposed to environmental pollutants all pose varying degrees of risk. Some risks are simply unavoidable. Some we choose to accept because to do otherwise would restrict our ability to lead our lives the way we want. And some are risks we might decide to avoid if we had the opportunity to make informed choices. Indoor air pollution is one risk about which something can be done.

In the last several years, a growing body of scientific evidence has indicated that the air within homes and other buildings can be more seriously polluted than the outdoor air in even the largest and most industrialized cities. Other research indicates that people spend approximately 90 percent of their time indoors. Thus, for many people, the risks to health may be greater due to exposure to air pollution indoors than outdoors.

If too little outdoor air enters a home, pollutants can accumulate to levels that can pose health and comfort problems. Unless they are built with special mechanical means of ventilation, homes that are designed and constructed to minimize the amount of outdoor air that can "leak" into and out of the home may have higher pollutant levels than other homes. However, because some weather conditions can drastically reduce the amount of outdoor air that enters a home, pollutants can build up even in homes that are normally considered "leaky". [29]

Indoor air quality is the result of complex interactions among buildings, building systems and people. Over the past several decades, people's exposure to indoor air pollution has increased due to a variety of factors. These include:

- the construction of more tightly sealed buildings without sufficient air exchange;

- reduced ventilation rates to save energy;

- the use of synthetic building materials and furnishings;

- the use of chemically formulated personal care products;

- the use of pesticides and housekeeping supplies;

- the increased complexity of modern building systems; and

- building deterioration due to age, improper maintenance or design. [12]

1.1.2 The importance of modelling the indoor climate

The indoor air is something that people are exposed to during the major part of their lives. Most people spend most of their time in artificial climates such as work/home environments and transport vehicles [2,21,22]. Clean air in a room is an essential component for a healthy indoor environment. Air is considered to be polluted when it contains certain substances in concentrations high enough and lasting long enough to cause harm or undesirable effects. In indoor environments, particles are the main cause of air pollution and of adverse effects on human health [9]. It is a well-known fact that indoor pollution originates from indoor processes and from outdoors. This makes the Indoor Air Quality (IAQ) problems very complex. The personal exposure to contaminants is primarily affected by the ventilation airflow and that is the function of total airflow rate in a closed compartment (room) as well as local airflow behaviour [2]. Essentially, a human is exposed to the contaminants which are found in the occupied zone. If one considers that the heat sources generate convective plumes, which are also part of the indoor airflow field then the modelling of indoor pollution without sophisticated computer software tools is almost impossible. Cold draughts from windows, convective plumes from radiators, plumes above human heads and airflow created by air diffusers are combined to the total indoor airflow field. Most of the contaminants such as CO_2, SO_2, CO, NO_x etc. move in the same manner as the primary airflows and do not constitute an extra challenge for the modelling. [7]

1.1.3 The evaluation of IAQ

The evaluation of the performance of a ventilation system is estimating the IAQ in the breathing zone. The breathing zone is defined as the zone where a human occupant is taking breathing air, H = 1.5 – 1.8 m above the floor level. Additionally, the occupied zone is assessed as the whole volume of the room from H = 0 – 1.8 m. Occupied zone average values are primarily assessed for evaluating the thermal comfort which clearly affects the whole human body. That is the main reason why the contaminant concentration is primarily assessed by evaluating the breathing zone value, but other parameters are calculated on the whole occupied zone. [7]

1.1.4 Ventilation efficiency of contaminant removal

One of the most important measures of ventilation system performance is its ability to remove contaminants. To describe the efficiency of a ventilation system many different quantities are used to evaluate the system performance. The mean ventilation efficiency, ε_c, in the room is defined as

$$\varepsilon_c = \frac{C_{out} - C_{in}}{\overline{C}_R - C_{in}}$$

(1)

where

C_{out} – concentration at exhaust opening (kg/m^3)

$\overline{C}_R$ – mean concentration in the room, (kg/m^3)

C_{in} – concentration at supply opening (kg/m^3)

1.1.5 Concentration

The concentration in the room, C_R, or given volume, corresponds to the amount of air which is contaminated by harmful gases. The concentration is highest close to the source. Concentration can be expressed in two ways, the first option is to use the contaminant source, m, or it can be expressed by using a room volume and the amount of harmful contaminant in the same volume.

3

$$C_R = \frac{\rho_p \dfrac{\pi d^3}{6} N}{V} = \frac{m/_{dt}}{V/_{dt}} = \frac{m}{Q_{out}} \tag{2}$$

ρ_p – particle density (kg/m3)

d – particle aerodynamic diameter (m)

N – number of particles in the room (nd)

m/dt – mass of particles produced in a room, later replaced by m (kg/s)

V/dt – volumetric flow rate in a room (m³/s)

1.1.6 Heat removal efficiency

The heat removal efficiency, ε_T, equation is defined by measuring or modelling the average temperature in the occupied zone, $\overline{T}_{OZ}$ (K), as well as in supply, T_{in} (K), and exhaust air, T_{out} (K).

$$\varepsilon_T = \frac{T_{out} - T_{in}}{\overline{T}_{OZ} - T_{in}} \tag{3}$$

1.1.7 Draught

If one considers thermal comfort and people's well-being in a ventilated room the effect of draught, DR (%), should be taken into account. Another good feature of following equation is the coupling of temperature, velocity and turbulence values into one equation. Fanger et.al [9] author suggested DR for calculating the draught rate, i.e. PPD (percentage of people dissatisfied) due to draught as follows,

$$DR = \left(3.143 + 0.37\overline{v}_{OZ}Tu_{OZ}\right)\left(34 - \overline{T}_{OZ}\right)\left(\overline{v}_{OZ} - 0.05\right)^{0.62} \tag{4}$$

where $\overline{T}_{OZ}$ is the air temperature, $\overline{V}_{OZ}$ (m/s) is the air velocity ($\geq$ 0.05 m/s) and Tu_{oz} (%) is the turbulence intensity in the occupied zone, respectively. Turbulence intensity is defined as (δ/v_{oz}) x 100%, where δ is the standard deviation of the air velocity. Draught rate is a parameter analysis to evaluate how closely the draught rating is associated to the heat and contaminant removal efficiency.

1.1.8 Other comfort evaluation equations

The occupant appreciates the indoor climate by its air quality and thermal conditions. The prediction of thermal sensation of indoor climate can be achieved by an index called Predicted Mean Vote (PMV) developed by[8].[7]

1.2 CONTAMINANTS

Mold, carbon monoxide and radon are the most serious contaminants affecting in rooms.

1.2.1 Mold

Molds are fungi that grow in damp environments. Mold spores contain allergens and irritants that often cause people living in houses where molds grow to suffer from allergic reactions and respiratory diseases.

Humid or damp conditions in your home can encourage the growth of mold and dust mites. Mold can develop from poor ventilation, flooding and building leaks. It can also grow in humidifiers, air conditioners, refrigerator drip pans and damp basements, on bathroom surfaces and behind furniture placed against outside walls or window frames. Moldy smells from basements, carpets and gypsum board are a sign that they harbour fungi.

1.2.2 Carbon Monoxide

Carbon monoxide is a colourless, odourless gas produced by the incomplete burning of any material containing carbon, such as propane, gasoline, oil, natural gas, coal or wood.

Possible sources of carbon monoxide in the home are:

- gas and oil furnaces and appliances that are not properly maintained or vented to the outside of the building;
- car engines in attached garages; and
- tobacco smoke.

The first symptom of carbon monoxide poisoning is usually a headache with throbbing temples. Other initial symptoms are tiredness and shortness of breath, tightness across the forehead, flushed skin and slightly impaired motor skills.

As the carbon monoxide level or exposure time increases, symptoms become more severe: irritability, chest pain, fatigue, diminished judgment, dizziness and dimness of vision. Still higher levels cause fainting upon exertion, marked confusion and collapse. If exposure continues, coma, convulsion and death from respiratory arrest can result.

1.2.3 Radon

Radon is a colourless, odourless radioactive gas that occurs naturally in our environment. It comes from the natural breakdown (radioactive decay) of uranium. Radon can be found in high concentrations where soils and rocks contain uranium, granite, shale or phosphate. Radon may also be found in soils contaminated with certain types of industrial waste, such as the by-products of uranium or phosphate mining [12].

1.2.4 Industrial contaminants

In Industries flue gases, CO, CO_2, SO_2 etc, will present which will act as contaminants by increase the density of air. In this work these contaminants are taken into account.

1.2 PRESENT WORK

In this thesis the main focus is the influence of air Velocity, temperature and contaminant concentration in a control panel room. Computer modelling is a vital part of everyday design in a building project. CFD modelling gives an opportunity to assess the indoor climate by virtually constructing a room and testing different system layouts to meet the predetermined design criteria.

Simulating only one part implies the risk that the designed system meets the requirements of, for instance, air velocity level in a human occupied zone, but fails to remove harmful pollutants. Typically the IAQ (indoor air quality) is assessed by means of total airflow supplied to the room, which should not be the only considered parameter in room ventilation because the air supply method and room internal configuration as well as heat sources have considerable effects on room air diffusion.

The goal for the project is to study the effect of contaminant temperature in control panel and effect on connected room. To perform a high-quality CFD particle simulation one needs to have broad knowledge associated to the inlet boundary conditions, wall boundary conditions and other boundary conditions in conjunction with operating a particle model within the CFD.

In this project air with different density is used as contaminant which is flowing at 50^0C.

2.1. COMPUTATIONAL FLUID DYNAMICS (CFD)

CFD is the systematic application of computing systems and computational solution techniques to mathematical models formulated to describe and simulate fluid dynamic phenomena.

CFD is part of computational mechanics, which in turn is part of simulation techniques. Simulation is used by engineers and physicists to forecast or reconstruct the behaviour of an engineering product or physical situation under assumed or measured boundary conditions (geometry, initial states, loads, etc.). A variety of reasons can be cited for the increased importance simulation techniques have achieved in recent years:

- Need to forecast performance
- Cost and/or impossibility of experiments
- The desire for increased insight
- Advances in computer speed and memory (1:10 every 5 years)
- Advances in solution algorithms

The simulation of flows is accomplished by:

- Solving numerically partial differential equations (PDEs),
- Following the interaction of a large numbers of particles, or
- A combination of both.

CFD, by its very nature, encompasses a variety of disciplines, which may be enumerated in the following order of importance:

- Engineering
- Physics
- Mathematics
- Computer Science (algorithms, coding, software)
- Visualization Techniques
- User Community (benchmarking, documentation, teaching)

2.1.1. The nature of CFD

CFD is a technique for predicting quantitatively:

- the performance of equipment,
- the behaviour of the:
  - o man-made
  - o natural environments,
- in circumstances involving:
  - o the flow of fluids
  - o the transfer of heat
  - o associated phase changes, and
  - o other concomitant effects [28]

Fluid flows play an important role in various equipment and processes in the industry. In general, information about the structure of the flow in a process or an apparatus can be obtained from measurements in experimental test facilities or from flow visualization studies. Although these techniques have proven to be of great importance, there are also limitations and a full picture of the flow field is often hard to obtain in this way. Computational Fluid Dynamics, commonly abbreviated as CFD, is a technique to model fluid flow using a computer simulation. Due to the recent rapid grow of powerful computer resources and the development of general purpose CFD software packages CFD can nowadays be applied to solve industrial flow problems. CFD has already proven to be a valuable tool to complement experimental findings in flow structure studies. In a computational simulation the flow structure is computed by solving the mathematical equations that govern the flow dynamics. The result is a complete description of the three-dimensional flow in the entire flow domain in terms of the velocity field and pressure distribution, including profiles of temperature variations, density and other related physical quantities. CFD codes include in their basic flow computations effects of heat and mass transfer and a range of physical and chemical models.

Applying CFD to industrial flow problems in the past has been of limited value, mainly because of the complexity of the flow geometries. Fortunately, today's CFD solvers have been designed to deal with geometries of any arbitrary structure. To perform a numerical simulation the flow geometry has to be represented by a computational mesh consisting of a large number of computational cells (representing the elements in the popular family of Finite Volume Methods). The flow field is solved in all these cells according to the conservation equations describing the flow dynamics. The accuracy and resolution of the results obtained depend on the number of cells defined: using more cells yields more details of the flow field on the expense of more computational effort (i.e. computer memory and CPU-time).[6]

2.1.2. PHOENICS

In the present paper a commercial CFD code PHOENICS developed and marketed by Cham has been used. A brief introduction regarding this code has been given in this section.

PHOENICS solves the conservation equations of air mass, momentum, energy, concentration, kinetic energy and dissipation rate of kinetic energy.

It can be used for the calculations of the distributions of room air velocity, temperature and helium concentration. The computation method involves the solution, in finite-domain form, of three-dimensional equations for the conservation of mass, momentum, energy, concentration, turbulence energy and dissipation rate of kinetic energy, with wall function expression for solid boundary conditions. The governing equations can be expressed in a single form:

$$div\left(\rho \vec{V} \phi - \Gamma_\phi grad\phi \right) \tag{5}$$

Where ϕ stands for any one of the following: 1, $u,v,\omega,\kappa,\varepsilon$,H and C. When ϕ =1, the equation changes into the continuity equation. A complete description of the theoretical basis can be found [27, 25, 19].[26]

PHOENICS, operated by its users, performs three main functions:

1. **Problem definition**, in which the user prescribes the situation to be simulated and the questions to which he wants the answers;

2. **Simulation**, by means of computation, of what the laws of science indicate will probably take place in the prescribed circumstances;

3. **Presentation** of the results of the computation, by way of graphical displays, tables of numbers, and other means.

PHOENICS, like many but not all CFD codes, has a distinct software module of the above three functions. This sub-division allows functions (1) and (3), say, to be performed on the user's home computer, while the power-hungry function (2) is carried out remotely.

PHOENICS simulates the prescribed physical phenomena by:-

- expressing the relevant laws of physics and chemistry, and the "models" which supplement them, in the form of equations linking the values of pressure, temperature, concentration, etc which prevail at clusters of points distributed through space and time;

- locating these point-clusters (which constitute the computational grid) sufficiently close to each other to represent adequately the continuity of actual objects and fluids;

- solving the equations by systematic, iterative, error-reduction methods, the progress of which is made visible on the VDU screen;

- enabling the computations to be interrupted, and the controlling settings to be modified, as the user desires;

- terminating when the errors have been sufficently reduced.[29]

2.2. NUMERICAL SIMULATION OF IAQ PARAMETERS BY CFD

Numerical methods by means of CFD modelling are used. CFD calculation represents a superior method to calculate the indoor airflow, because semi-empirical and purely analytical methods fail for different room layout

conditions. The temperature or contaminant gradients and convection flows from heat sources could be calculated by models developed by [23,17], but these models are not applicable in all room layout situations. Basically because of these restrictions, the use of CFD as a universal tool to predict indoor airflows has grown dramatically. Another significant advantage of CFD is the possibility to test different system configurations virtually without constructing the real systems.

2.3 GENERAL BOUNDARY CONDITIONS

The CFD simulations performed in the present work are carried out in 3D space with steady-state conditions using the commercial code PHOENICS. Discretisation of pressure was always of second order accuracy. The momentum and energy were always discretised in a second order upwind scheme [22]. Turbulent kinetic energy, k, and turbulence dissipation rate, ε, were in most cases solved by first order upwind accuracy.

2.4 FLUID DYNAMICS THEORY

2.4.1 Laminar flow equations

For airflows, the CFD program solves conservation equations for mass and momentum. For flows involving heat transfer or compressibility, an additional equation for energy conservation is solved. Two additional transport equations are solved when the flow is turbulent, i.e. the turbulent transport quantities k and ε in the k-ε model. [7]

2.4.1.1 Mass conservation equation

The equation for conservation of mass, or continuity equation at steady state, can be written as follows:

$$\nabla\left(\vec{v}\,\rho\right) = 0 \tag{6}$$

12

Above equation is the general form of the mass conservation equation and is valid for incompressible as well as compressible flows, where $\vec{v}$ the velocity vector and ρ is the fluid density.

2.4.1.2 Momentum conservation equation

The momentum equation can be expressed by Navier-Stokes equations by describing Newton's second law of fluid flow. The momentum equation can be expressed in vector form as

$$\nabla \cdot \left(\rho \vec{v} \otimes \vec{v} \right) = \nabla \cdot \left(\mu_{tot} \nabla \vec{v} \right) - \nabla p + \vec{F}_g + \vec{F}_{\Delta T} \tag{7}$$

where $\vec{v}$, ρ, p (Pa), $F_{\Delta T}$ (N) are the velocity vector, density, pressure and thermal differences in the buoyancy term, respectively. It is worth mentioning that in turbulent flow the viscosity, μ_{tot} (kg/ms), is the sum of molecular and turbulent viscosity. Natural convection is modelled by the Boussinesq approximation.

2.4.1.3 Energy conservation equation

To obtain a description of the temperature distribution throughout the non-isothermal flow domain the energy equation is used. Energy, E, in the air is defined as the sum of internal thermal energy, kinetic energy of velocity components and the gravitational potential energy typical in buoyancy-driven flows. Conservation of energy at steady state is described by

$$\nabla \cdot \left(\vec{v}(\rho E + p) \right) = -\nabla \cdot \left(\sum_j h_j J_j \right) + S_h \tag{8}$$

where J_j is the diffusion flux of species j (kg/m^{2}s), h_j is the enthalpy (kJ/kg) of species j and S_h (W/m^3) includes the heat or any other volumetric heat sources defined in the simulation process.[7]

2.4.2 Turbulent flow equations

The mean-value theory equations are obtained for the velocity components as

$$U = \overline{U} + u'$$
$$V = \overline{V} + v' \tag{9}$$
$$W = \overline{W} + w'$$

The density and pressure may also be represented in the same way. However, any changes in density are assumed to be the result of temperature changes within the flow field.

2.4.2.1 Turbulent Flow Equations – Continuity

If the velocity expressions of Eq (9) are substituted into the continuity equation, the following equation results after a time average is taken.

$$\frac{\partial \overline{U_i}}{\partial X_i} = 0 \tag{10}$$

Subtracting Eq(8) from continuity equation

$$\frac{\partial U_i'}{\partial X_i} = 0 \tag{11}$$

Thus, both the mean and fluctuating velocity components must individually satisfy the continuity equation. It is important to note that these equations are based strongly on the assumption that no turbulent density fluctuations exist. For most practical flow situations, it is generally sufficient to ignore Eq (11) and focus only on the continuity equation of the mean flow [13].

2.4.2.2 Turbulent Flow Equations – Momentum

If the velocity expressions of Eq(9) are substituted into the momentum equation, and a time average is taken, the following equation will result.

14

$$\frac{\partial \overline{U_i}}{\partial t} + \frac{\partial}{\partial X_j}(\overline{U_i U_j}) + \frac{\partial}{\partial X_j}(\overline{U_i' U_j'}) = -\frac{\partial}{\partial X_i}\left(\frac{P}{\rho}\right) + g_i + \upsilon \nabla^2 \overline{U_i} \qquad (12)$$

Eq(12) may be manipulated slightly to distinguish the right-hand side of the equation as containing both viscous and turbulent (Reynolds) stresses as shown by the following equation.

$$\rho\frac{\partial \overline{U_i}}{\partial t} + \rho\frac{\partial}{\partial X_j}(\overline{U_i U_j}) = -\frac{\partial P}{\partial X_i} + \rho g_i + \frac{\partial}{\partial X_j}(\mu\frac{\partial \overline{U_i}}{\partial X_j}) + \frac{\partial}{\partial X_j}(-\rho\overline{u_i' u_j'}) \qquad (13)$$

The fact that these Reynolds stresses consist of correlations of velocity fluctuations render the stresses impossible to solve. This incapacity to predict the correlations is known as the "Closure Problem." As a result, exact solutions are not possible.[16]

2.4.2.3 Turbulence modelling with the k-ε model

Air movements in a room are usually turbulent and need be modelled in CFD. In turbulent flow we can divide the variables into one time-averaged part of the velocity $\bar{v}$ (when the mean flow is steady) and one fluctuating part v, so that $\bar{v}+v$. In the standard k-ε model the modelled transport equations for turbulent kinetic energy, k, and its dissipation rate, ε, are solved. The present model assumes that the flow is fully turbulent and the effects of molecular viscosity are small compared to the turbulent viscosity, $\mu_{tot} = \mu + \mu_{turb}$. That is why this model is very suitable for fully turbulent flows and it calculates the turbulence isotropically. That is why the anisotropic flows such as wall jets should be calculated with other turbulence models. Turbulent viscosity in this model is computed as

$$\mu_{turb} = C_\mu \rho \frac{\kappa}{\varepsilon} \qquad (14)$$

In transport equations of k and ε one need values for 5 unknown constants [4]. Unfortunately these constants are not universal for all types of flows. The present thesis used default values, $C_{1\varepsilon}$ − 1.44; $C_{2\varepsilon}$ − 1.92; C_μ − 0.09; σ_k − 1.0; σ_ε − 1.3.

When using k-ε model modifications the default values provided [9] were used as well. More information about the standard k-ε turbulence model can be found in numerous publications [5, 19, 30]. Other turbulence models are not discussed in this thesis, but quite broad knowledge about different turbulent models within CFD is given by [5].

If the Navier-Stokes equations are solved without using any approximations in turbulence modelling, the approach is called DNS (direct numerical simulation). Successful prediction with DNS needs a very fine mesh to capture all the smallest eddies in the flow. The smallest eddy size in the turbulent flow is of the order of the Kolmogorov length scale l_k (m).u7

$$l_k = \left(\frac{V}{\varepsilon}\right)^{0.25} \tag{15}$$

where v is the kinematic viscosity of air. For most of indoor airflow the Kolmogorov length scale is around 0.01 to 0.001 m. To use the DNS method the grid number for the simulation is very high and not feasible in today's PC.[7]

2.4.2.4 RNG Theory of turbulence

The incompressible Navier-Stokes equations are

$$\nabla . v = 0, \tag{16}$$

$$\frac{\partial v}{\partial t} + v.\nabla . v = -\frac{1}{\rho}\nabla p + v_0 \nabla^2 v, \tag{17}$$

where v_0 is the (constant) molecular kinematic viscosity. The problem at hand is to construct a turbulence theory for flows at large Reynolds numbers. The 1987 paper by Yakhot and Orszag [31] first applied the renormalization group (RNG) technique to high Reynolds number turbulent flows, following the basic ideas in the 1976 and 1977 works of Forster, Nelson and Stephen [11] on fluctuations in a randomly stirred fluid. Several unconventional artifices were used in the theoretical developments. First, following Forster, Nelson and Stephen, a scale invariant random force f with certain statistical properties was inserted into the Navier-Stokes equations via the correspondence principle, which postulated that

16

solutions forced solely by this special f were "statistically equivalent... in the inertial range" to the unforced solutions for problems with nontrivial initial and/or boundary conditions. Second, an ε-expansion procedure was used extensively when the value of the artificially introduced expansion parameter, ε, was 4.

2.4.2.4.1 The Boussinesq Postulate

The traditional approach to turbulence is to divide the flow variables into a mean part and a fluctuating part with zero mean:

$$v = v_0 + v', \quad p = p_0 + p'. \tag{18}$$

Substituting (18) into (16) and (17), and taking the appropriate time average, equations identical to (16) and (17) are obtained except the laminar stress term in (17) is augmented by the addition of a turbulent stress, $-\langle v'v' \rangle$. To determine this turbulent stress [1] assumes the mean turbulent stress can be expressed approximately in the same form as the laminar stress with a turbulent kinematic viscosity, ν_T

$$\text{turbulent stress} \approx \rho\nu_T \left[\nabla v_0 + \left(\nabla v_0\right)^T \right] \tag{19}$$

Determination of a single scalar problem is reduced if Boussinesq postulate is accepted. In principle, once a theory for ν_T is developed, the problem for the mean flow is solved. Since ν_T is obviously dependent on the characteristics of the fluctuating part of the solution, the two parts are coupled, and both must be given appropriate theoretical attention.

2.4.2.4.2 Theory of Turbulence

The Yakhot and Orszag RNG theory of turbulence begins by postulating the correspondence principle which inserts a divergence-free isotropic random force into (17):

$$\frac{\partial v}{\partial t} + v.\nabla v = -\frac{1}{\rho}\nabla p + \nu_0\nabla^2 v + f, \tag{20}$$

17

where f is "chosen to generate the velocity field described by the (Kolmogorov) spectrum...in the limit of large wave number k." The correlation function of the random force f chosen by Yakhot and Orszag is

$$\left\langle {}^{\wedge}f_i(\mathbf{k},\omega)^{\wedge}f_j(\mathbf{k}',\omega')\right\rangle = 2D_0^*(\varepsilon,k)k^{-d}(2\pi)^{d+1}\left(\delta_{ij} - k_ik_j / k^2\right)\times \delta(\mathbf{k}+\mathbf{k}')\delta(\omega+\omega'),\quad (21\text{a})$$

where ${}^{\wedge}f_i$ is the space-time Fourier transform of f, k is wave number, w is frequency, d is the dimension of the physical space, and $D_0^*(\varepsilon,k)$ which has the dimension of velocity squared per unit time, is expressed as a product of two factors according to their k dependence:

$$D_0^*(\varepsilon,k) \equiv D_0(\varepsilon)(k)^{4-\varepsilon}, \qquad \text{(dimension = velocity squared/time)}. \qquad (21\text{b})$$

Here $D_0(\varepsilon)$ and k (the magnitude of k) are both dimensional, and ε is a dimensionless parameter. The Yakhot and Orszag theory assumed $D_0(\varepsilon)$ to be independent of any characteristic length scale, especially the user-specified ultraviolet cutoff wave number Λ.

The logic of RNG theory can be described as follows. In turbulent flows, the energy spectrum of the small turbulent eddies naturally decays exponentially for $k \geq \Lambda_0$, where Λ_0 is a large ye-dependent "dissipation" ultraviolet cutoff wave number. So, if all the $k > \Lambda_0$ Fourier components of an exact solution were removed, the filtered solution in physical space-time would be little affected and would still satisfy the same original Navier-Stokes equations approximately. In the so-called inertial range $\Lambda_0 \geq k \geq 1/L$, the magnitude of the energy spectrum becomes significant and is expected to follow the Kolmogorov scaling law-provided the Reynolds number is sufficiently large. If a narrow band $\Delta\Lambda$ at the ultraviolet edge $\Lambda_0 \geq k \geq \Lambda_0 - \Delta\Lambda$ were filtered out, the filtered solution would now be significantly affected, and would no longer satisfy the original Navier-Stokes equations. The filtering process generates new terms. The RNG theory, obviously prompted by the Boussinesq postulate, uses a correction $\Delta\nu$ to ν_0 to

18

absorb the major effects of these new terms at low k and w. By recursively filtering the solution, the value of the user- pecified ultraviolet cutoff wave number A can be moved downward to some lower value in the inertial range, while the value of $v_T(\Lambda)$ increases by accumulating the corrections from Δv to some much larger value. The residual of the new terms not absorbed by the Δv correction also accumulates.

In spite of the fact that ε was required to be 4, Yakhot and Orszag applied the so-called ε-expansion procedure in the derivation of v_T, and argued that the residual new terms (beyond those already accounted for by v_T) in the modified Navier-Stokes equations for the filtered solution could be ignored because they were "higher order" in ε. The "lowest-order" theory, [31,4] when supplemented by an appropriate closure assumption, yielded a number of scaling law constants.

2.4.2.4.3 Dimensional Analysis

In general, the RNG theory of turbulence contains five dimensional input parameters: a characteristic physical length scale L, a characteristic velocity U, the molecular kinematic viscosity v_0, the dimensional $D_0(\varepsilon)$ factor in the random force, and the artificial ultraviolet cutoff wave number Λ. Under the assumptions that the Reynolds number is sufficiently large ($UL/v_0 \geq 1$), the artificial ultraviolet cutoff is sufficiently high ($\Lambda L \geq 1$), and that the characteristic time scale of the problem is sufficiently long in comparison the time scales of the small eddies

$$\left(L/U \geq \left[D_0^*(\varepsilon, \Lambda) \right]^{\frac{1}{3}} (\Lambda)^{-\frac{2}{3}} \right)$$ the dynamics of the small turbulent eddies is expected

to behave in some universal manner; its weak dependence on U, L, and v_0 can be ignored altogether. Under these conditions, $D_0(\varepsilon)$ and Λ are the only dimensional input parameters available.

The only possible form for v_T, the main dimensional output parameter, is the following:

$$v_T = \Pi_1 \left[D_0^*(\varepsilon, \Lambda) \right]^{\frac{1}{3}} (\Lambda)^{-\frac{4}{3}} = \Pi_1 \left[D_0(\varepsilon) \right]^{\frac{1}{3}} (\Lambda)^{-\frac{\varepsilon}{3}} \tag{22}$$

where Π_1, is a dimensionless constant.

Let $E(\Lambda)$ be the value of the energy spectrum at the user-specified ultraviolet cutoff $\Lambda \geq k_* = O\left(\frac{1}{L}\right)$ where k_* is the lower edge of the inertial range. The only possible form for $E(\Lambda)$ is

$$E(\Lambda) = \Pi_2 \left[D_0^*(\varepsilon, \Lambda) \right]^{\frac{2}{3}} (\Lambda)^{-\frac{5}{3}} = \Pi_2 \left[D_0(\varepsilon) \right]^{\frac{2}{3}} (\Lambda)^{1 - \frac{2\varepsilon}{3}} \tag{23}$$

where Π_2, is a dimensionless constant. Here Λ_0, is assumed to be infinite.

Let ε be tentatively identified with some relevant energy dissipation rate (with dimension velocity squared per unit time) of the unfiltered flow field. The only possible form for ε, assumed to be independent of k, is

$$\varepsilon = \Pi_3 \, D_0^*(\varepsilon, \Lambda) = \Pi_3 \, D_0(\varepsilon)(\Lambda)^{4 - \varepsilon} \tag{24}$$

where Π_3, is a dimensionless constant. Since ε must also be independent of Λ, (24) clearly indicates that $D_0(\varepsilon)$ is Λ dependent when $\varepsilon \neq 4$. It is useful to remark here that the innocent looking (24) is at the heart of the matter being addressed.

The immediate task of a turbulence theory is to determine the values of ε, Π_1,, Π_2, and Π_3,. The YO theory concluded from (23) that $\varepsilon = 4$ was needed to recover the Kolmogorov energy by spectrum. Actually, this conclusion is solely the consequence of assuming $D_0(\varepsilon)$ to be independent of Λ, and will be challenged. In what follows, ε will be kept symbolically in (24) without committing ε to any specific value. The scaling laws (22)-(24) all have ε-dependent exponents, and all involve $D_0(\varepsilon)$. For reasons which will become clear later, it is preferable to use ε instead. Using (24) to eliminate $D_0(\varepsilon)$ in favor of ε from (22) and (23) one obtains the following:

$$v_T = \pi_1 (\varepsilon)^{\frac{1}{3}} (\Lambda)^{-\frac{4}{3}} \tag{25}$$

$$E(\Lambda) = \pi_2 (\varepsilon)^{\frac{2}{3}} (\Lambda)^{-\frac{5}{3}} \tag{26}$$

where

$$\pi_1 = \Pi_1 \Big/ \Pi_3^{1/3} \tag{27a}$$

$$\pi_2 = \Pi_2 \Big/ \Pi_3^{2/3} = \text{denoted as } C_k \text{ in YO} \tag{27b}$$

Equation (26) is the Kolmogorov $E(k)$ in the inertial range, and it has been straightforwardly derived here by eliminating $D_0(\varepsilon)$ in favor of ε using (24). Many additional useful relations can be derived from (25) and (26). Eliminating ε between them, one obtains the following:

$$\pi_3 = [E(\Lambda)]^{-1}(\Lambda)(v_T)^2 = \Pi_1^2 \Big/ \Pi_2 = \pi_1^2 \Big/ \pi_2 \tag{28}$$

Eliminating Λ, one obtains

$$\pi_4 = [E(\Lambda)]^{-4/3}(\varepsilon)^{1/3}(v_T) = \Pi_3^{1/5}\,\Pi_1 \Big/ \Pi_2^{4/5} = \pi_1 \Big/ (\pi_2)^{4/3} \tag{29}$$

The kinetic energy $K(\Lambda)$ contained in all the eddies with $K > \Lambda$ in the inertial range is readily computed by integrating $E(k)$ as given by (26) from Λ to infinity while holding ε constant:

$$K(\Lambda) = \int_\Lambda^\infty E(k)dk = \frac{3}{2}\Lambda E(\Lambda) \tag{30}$$

Other interesting relations which appear in YO are

$$\pi_5 = [K(\Lambda)]^{-2}(\varepsilon)(v_T) = \frac{4}{9}\frac{\Pi_3\Pi_1}{\Pi_2^2} = \frac{4}{9}\frac{\pi_1}{\pi_2^2} = \text{denoted as } C_\nu \text{ in YO} \tag{31}$$

which is of particular interest in $K - \varepsilon$ modeling, and

$$\pi_6 \equiv (\varepsilon)(\Lambda)^{-3}[E(\Lambda)]^{-1}(v_T)^{-1} = \Pi_3 \Big/ \Pi_2\Pi_1 = 1 \Big/ \pi_1\pi_2 \tag{32}$$

$$\pi_7 \equiv (\varepsilon)(\Lambda)^{-2}[E(\Lambda)]^{-2}(v_T) = \Pi_1\,\Pi_3 \Big/ \Pi_2^2 = \pi_1 \Big/ \pi_2^2 \tag{33}$$

$$\pi_8 \equiv (\Lambda)^{-2}[K(\Lambda)](v_T)^{-2} = \frac{3}{2}\frac{\Pi_2}{(\Pi_1)^2} = \frac{3}{2}\frac{\pi_2}{(\pi_1)^2} \tag{34}$$

Only two of the above scaling law constants are independent. Most importantly, the dimensional analysis above does not care whether a random

21

force has in fact been inserted or not, nor does it have any interest in the details of the RNG and/or any associated solution algorithms. The critical physical assumption is that the only relevant dimensional parameters are Λ and ε. Note that once ε is used in place of $D_0(\varepsilon)$, the scaling laws no longer have ε-dependent exponents.[18]

2.4.2.4.4 LOW-REYNOLDS NUMBER (LRN)

One of the most important and least understood aspects of turbulence is that which occurs when the local Reynolds number of the turbulence is low. The presence of the wall ensures that over a finite region of the flow, however thin, the turbulence Reynolds number is low enough for molecular viscosity to influence directly the processes of production, destruction and transport of turbulence.

The hydrodynamic predictions have been obtained from the solution of the equations:

streamwise momentum,

$$\rho u \frac{\partial u}{\partial x} + \rho v \frac{\partial u}{\partial y} = \frac{\partial}{\partial y}\left(\mu \frac{\partial u}{\partial y} - \overline{\rho u' v'}\right) - \frac{dp}{dx} \tag{35}$$

turbulent viscosity hypothesis,

$$-\overline{\rho u' v'} = \mu_T \frac{\partial u}{\partial y} \equiv \left(c_\mu \rho k^2 / \varepsilon\right)\frac{\partial u}{\partial y} \tag{36}$$

turbulence kinetic energy,

$$\rho u \frac{\partial k}{\partial x} + \rho v \frac{\partial k}{\partial y} = \frac{\partial}{\partial y}\left[\left(\mu + \frac{\mu_T}{\sigma_k}\right)\frac{\partial k}{\partial y}\right] + \mu_T \left(\frac{\partial u}{\partial y}\right)^2 - \rho\varepsilon - 2\mu\left(\frac{\partial k^{1/2}}{\partial y}\right)^2 \tag{37}$$

turbulence dissipation rate

$$\rho\mu \frac{\partial \varepsilon}{\partial x} + \rho v \frac{\partial \varepsilon}{\partial y} = \frac{\partial}{\partial y}\left[\left(\mu + \frac{\mu_T}{\sigma_\varepsilon}\right)\frac{\partial \varepsilon}{\partial y}\right] + c_1 \frac{\varepsilon}{k}\mu_T\left(\frac{\partial u}{\partial y}\right)^2 - \frac{c_2\rho\varepsilon^2}{k} + 2.0\frac{\mu\mu_T}{\rho}\left(\frac{\partial^2 u}{\partial y^2}\right)^2 \tag{38}$$

Above system of differential and auxiliary equations which are well known and, with the exception of the last term appearing in it, so is the simulated form of

the turbulence energy Eq.37. The reasons for including this extra term are computational rather than physical; for, in solving the ε equation, there are decisive advantages, in letting ε go to zero at the wall. However, the turbulence dissipation rate is not zero there; it is in fact equal to

$$\mu\left[\overline{\left(\frac{\partial u'}{\partial y}\right)^2}+\overline{\left(\frac{\partial w'}{\partial y}\right)^2}\right]$$

(39)

ε-equation and k-equation are parallels and very closely as: each equation adopts the assumption that diffusional transport proceeds at a rate proportional to the product of the turbulent viscosity and the gradient of the property in question (the terms σ_k, and σ_ε thus have the significance of turbulent Prandtl numbers). Moreover the principal generation and decay terms (the former arising through mean velocity gradients) in the two equations are likewise similar.

To complete the specification of the model the quantities $C\mu$, C_1, C_2 σ_k and σ_ε must be prescribed. At high Reynolds numbers these are all supposed to take on the constant values given in k-ε turbulence model. Here $C\mu$ is fixed by the requirement that in a constant-stress layer $\tau_w/\rho k = c_\mu^{1/2}$; C_2 is determined by reference to the decay of grid turbulence; and C_1 is chosen so that the von Karman constant equals 0.42. The diffusion coefficients σ_k and σ_ε were fixed in [15] by computer optimisation.

At low Reynolds numbers two of these, $C\mu$ and C_2, become dependent upon the value of the turbulence Reynolds number, R_T, which we now quantity as the parameter ($\rho k^2 / \varepsilon \mu$). The functional dependences chosen are:

$$c_\mu = 0.09\exp(-2.5/(1 + R_T / 50))$$

(40)

$$c_2 = 2.0(1.0 - 0.3\exp(-R_T^2))$$

(41)

The parabolic partial differentials Eq.35 Eq.37 Eq.38 (or their equivalents for axisymmetric pipe flows) have been solved by means of an adapted version of the [20] finite-difference procedure.

At the wall both k and ε were set to zero. Provided the density is uniform, a complete specification of the hydrodynamic field is achived. When, however, the thermal field is of interest, the enthalpy conservation equation must also be solved. For fluids of uniform specific heat, the two-dimensional boundary-layer form of the equation may be written:

$$\rho u \frac{\partial T}{\partial x} + \rho v \frac{\partial T}{\partial y} = \frac{\partial}{\partial y} \left(\lambda \frac{\partial T}{\partial y} - \rho \overline{v'T'} \right) \tag{42}$$

where λ denotes the thermal conductivity divided by the specific heat at constant pressure. In consonance with Eq.36 the turbulence correlation appearing in Eq.42 is approximated as follows:

$$- \rho \overline{v'T'} = \lambda_T \frac{\partial T}{\partial y} \equiv \frac{\mu_T}{\sigma_h} \frac{\partial T}{\partial y} \tag{43}$$

The term σ_h which is the turbulent Prandtl number for enthalpy transport, is assigned the value 0.9, independent of Reynolds numbers, for all the heat-transfer calculations.[14]

2.5 CFD MODELLING OF THE AIR AND CONTAMINANT DISTRIBUTION IN ROOMS

Computational fluid dynamics (CFD) modelling and scale (or physical) modelling are, in principle, the two alternative approaches for evaluating the global indoor environments with the .aim to obtaining a proper design of building service systems. Both approaches have their advantages and limitations. CFD has, nevertheless, become a widely accepted alternative to the scale modelling in recent twenty years for predicting the air motion in buildings and indoor air quality.

The k-ε model has been used worldwide since it was created. However, for the HRN model, the so-called wall function must be properly designed to correlate the physical parameters between the LRN and HRN flow zones. It has so far been believed that the wall function has a large influence on the heat

transfer near to the solid boundaries. Thus, the problem is now to find the correct wall function if it is needed. In addition, for the LRN model, the relationship between turbulent coefficients and turbulent Reynolds number was not totally known until now. About k-ε model we have studied in turbulent flow.

Calculation of the partial differential equations:-

For solving the governing equations of air and contaminant motion in room(s), Baker et al. [8] recently presented a new method, called the Taylor Weak Statement (TWS).Similar to the method of weighted residuals.

The sum of the residual (TWS) over a sub-domain (control volume or element) of interest be minimized as follows

$$TWS = \int_{\Omega} \phi_i(\bar{x}) L^c(q^N) d_\tau = 0 \tag{44}$$

q^N which contains a number of undetermined parameters

From the foregoing introduction of the TWS method, it can be found that the weighted residual method was executed to a resultant PDE by introducing an artificial diffusive term to the governing PDEs the stability of the solution can be improved by this diffusive term. This term causes a filtering effect to the high frequency fluctuation of air flow

Modelling of Air Terminal Devices (ATD) in room:-
Momentum similarity at ATD:-

A complicated diffuser is modelled by a simple opening which lets the supply air have the same momentum and same direction as reality. Two versions to the basic approach exist. In the first, a simple opening has the same effective area as the real diffuser, then the same velocity as each nozzle. The second version lets the momentum force defined by Eq. (45) and the supply air direction be the same between the simple opening and the complicated diffuser. The opening area can, somewhat freely, be chosen.

25

$$F = \int \rho U^2 dA \qquad (45)$$

Momentum similarity in front of the ATD:-

This approach is based on well-developed wall-jet techniques. The air velocity field within a small space in front of a diffuser is self-similar. Thus, the momentum similarity of the ATD can be defined away from the ATD by using the well-developed wall-jet technique. This method is more difficult. However, it was believed that better results could be achieved.

Wall function:-

The wall function was originally a method to deal with the boundary conditions for the HRN model. The HRN model was based on the assumption that the R_t value is so high that the turbulent parameters C_1, C_2, C_μ and C_3 could be treated as constant. This assumption does not hold in the region near the solid boundaries at any time. Hence, a 'known' function (so-called wall function), is needed to connect the boundary conditions with the physical parameters in the domain The Velocity and Temperature Distributions (VTD) of the fiat plate boundary layer flow or the Couette flow have been selected as the wall function. wall function by dividing the boundary layer into three regions, the viscous sublayer, buffer zone and fully turbulent log-law zone then evaluated the VTD by using different formulas for each region. The differences between computed and measured convective heat transfer coefficient to about 20%, but it is high. The velocity distribution in the whole boundary layer over a flat plate had been deduced by Spalding [19] more than 30 years ago, which is expressed by Eq. (46).

$$y^+ = u^+ + 0.1108 \times \left[\exp^{0.4u^+} - 1 - 0.4u^+ - \frac{(0.4u^+)^2}{2} - \frac{(0.4u^+)^3}{3} \right]$$

$$u^+ \equiv u(\rho/\tau_w)^{1/2}; y^+ \equiv y(\tau_w \rho/\mu)^{1/2} \qquad (46)$$

The air flow over the walls is seldom in parallel to the wall surface. Therefore, each wall function, in fact, is based on the assumption that the flow is

similar. Hence, any model plus the wall function has more or less the same difficulties as the mixing-length model. The LRN model has phased out the usage of the wall function. Though it still has some problems that have not yet been solved, it offers an opportunity to handle the room air flow.

Concluding remarks:-

The k-ε model in simulating the room air flow was reviewed. It was concluded that the turbulent parameters should be functions of the turbulent Reynolds number even in the case where the wall function was to be used. It is evident that the air flow in modem buildings is very slow.

ATD method shows the benefit from evaluating the jet decay, but the prediction on jet spread and thickness may be far from reality. This could be indicated by unbelievably uneven computed temperature and contaminant distributions. Further research is required [32].

2.6 MEASUREMENTS AND COMPUTATIONS OF VENTILATION EFFICIENCY AND TEMPERATURE EFFICIENCY IN A VENTILATED ROOM

In order to improve the indoor air quality in a room and to save energy, the air movement and contamination distributions in the room with ventilation have been studied experimentally and numerically. The measurements concern room airflow pattern and air temperature, velocity and contamination concentration fields, etc. The reduction of the ventilation rate causes an increase of the concentration of indoor air contaminants. Due to the decrease of mechanical ventilation, the airflow in office buildings has changed from a forced into a mixed convection. Buoyancy becomes one of the dominant factors of indoor airflow.

The experiments were carried out in a full scale climate room which is 5.6 m long, 3.0 m wide and 3.2 m high. In this room, four kinds of ventilation systems were used.

--System 1: an inlet air diffuser 68 cm high and 50 cm wide was located on the floor near the rear wall. Two outlets were in the rear wall near the ceiling. A table 175 cm long, 145 cm wide and 85 cm high was placed near the window.

-- System 2: the air diffuser was installed on the floor near the window and there were two outlets in the rear wall near the ceiling. In this system, the table cannot be placed near the window otherwise the inlet air is confined under the table.

--System 3: two vertical jets were installed on the floor near the window. The inlet size for both of them was 100 cm long and 1 cm wide. Two outlets were in the rear wall near the ceiling. The table was located near the window.

-- System 4: two horizontal jets in the upper part of the rear wall were used. The inlet size of each was 25 cm long and 2 cm high. Two outlets were in the rear wall near the floor.

The experimental and computational results of room airflow, temperature and contamination distributions will be reported in three groups:
(1) different ventilating systems;
(2) different ventilation rates;
(3) different heat gains from the Venetian blinds.

Here both PHOENICS and ACCURACY are used, because PHOENICS solves the conservation equations of air mass, momentum, energy, concentration, kinetic energy and dissipation rate of kinetic energy. ACCURACY, which considers the influence of room air temperature distributions, is employed for the determination of cooling load, wall surface temperatures and convective heat transfer on room enclosure surfaces. These are the boundary conditions required by PHOENICS.

Results have been concluded that
(1) Most of the computations presented in this paper are in good agreement with the measured results. A few discrepancies were found.

(2) The temperature and ventilation efficiencies of systems 1 and 2 are very high. They seem to be the best ones both for saving energy and obtaining good air quality in cooling situations. However, system 2 is not as good as system 1. System 3 presents higher ventilation efficiency but is not easy to control. System 4 is a representative of commonly used systems where room air is perfectly mixed. Its temperature and ventilation efficiencies are very low.

(3) According to the results of system 1, the higher the ventilation rate, the larger the temperature efficiency and the ventilation efficiency and the smaller the temperature gradient. In addition, the energy consumption also depends on the ventilation rate. Obviously, it is easier to remove the contaminant in the case with a high ventilation rate.

(4) The larger the amount of heat introduced on the venetian blinds for system 1, the lower the ventilation efficiency and the larger the temperature gradient. Its influence on temperature efficiency is small.

(5) If room heat gain and ventilation rate are the same, the required inlet air temperature of the four systems is different. In cooling situations, the supplied inlet air temperature of systems 1 and 2 can be higher than that of system 4. This has to be considered in building energy analysis. The computer program ACCURACY can be employed for this purpose. A new calculating method is suggested. [26]

System Configuration:-

A system is designed to study the flow of contaminants, temperature, air velocity and pressure profiles. It is an industrial control panel room connected with a rest room.

The control panel room has one inlet, one outlet and a door. Air flows into the room at a rate of 0.1m/s through the inlet and output works on pressure difference.

The rest room which is adjacent to control panel room has one inlet (outlet of control panel room), one outlet and a door. These rooms are designed in such a way that the inlet of control panel is above the plant roof.

Due to some leakage in the (which acts as a point source) control panel, the flue gas at 50°C temperature from plant enters into the room. This is considered as contaminant.

An increase in contaminant concentration or temperature will affect the Indoor Air Quality.
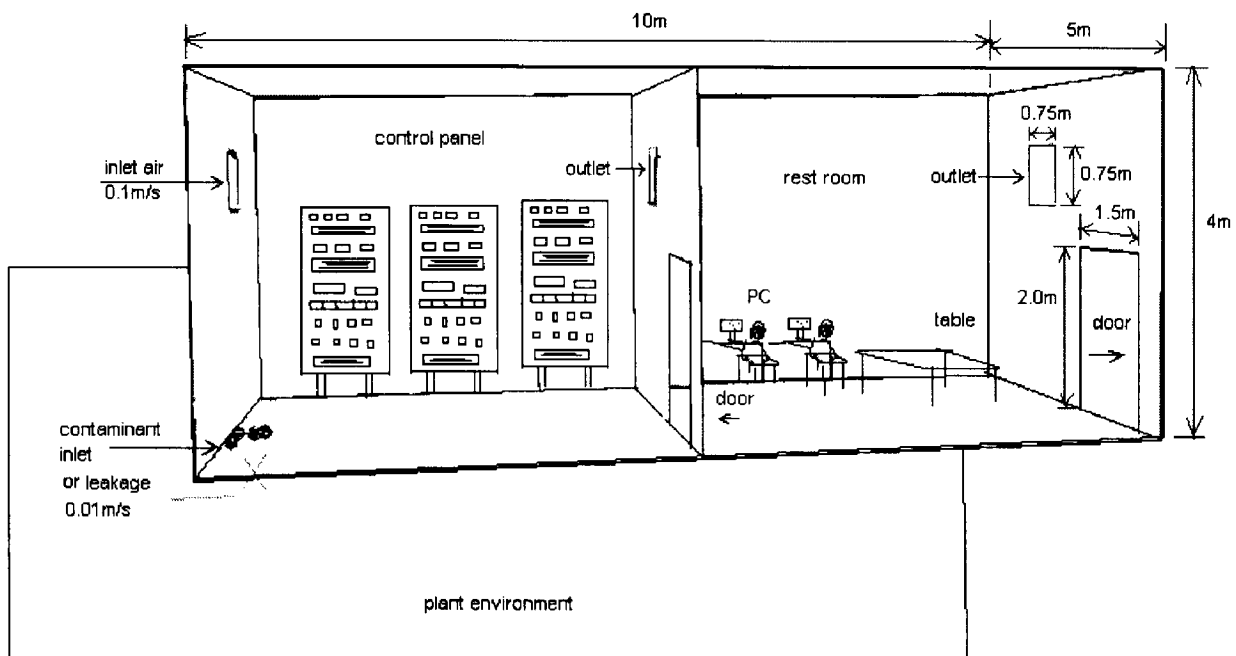
Fig.1 Schematic diagram of model

The flow modeling is carried out to focus on stationary characteristics with a view to assess indoor air quality and thermal comfort. Analysis of the energy use of a room or a building however requires information on the transient characteristics of the indoor climate.

A flow field can be described by the conservation of mass, momentum and energy. Given the boundary conditions, the resulting flow pattern is determined by solving the combined Navier-Stokes and energy or any other scalar equations.

4.1 MATHEMATICAL MODEL:

4.1.1 CONTINUITY EQUATION:

$$\frac{\partial}{\partial x_1}(u_1) = 0 \tag{47}$$

$$\frac{\partial}{\partial x_2}(u_2) = 0 \tag{48}$$

$$\frac{\partial}{\partial x_3}(u_3) = 0 \tag{49}$$

4.1.2 MOMENTUM BALANCE:

$$\frac{\partial}{\partial t}(u_1) + \frac{\partial}{\partial x_1}(u_1 u_1) = -\frac{\partial}{\partial x_1}\left(\frac{p}{\rho} + \frac{2}{3}k\right) + \frac{\partial}{\partial x_1}\left[\vartheta_t\left(\frac{\partial}{\partial x_1}(u_1) + \frac{\partial}{\partial x_1}(u_1)\right)\right] \tag{50}$$

$$\frac{\partial}{\partial t}(u_1) + \frac{\partial}{\partial x_2}(u_1 u_2) = -\frac{\partial}{\partial x_1}\left(\frac{p}{\rho} + \frac{2}{3}k\right) + \frac{\partial}{\partial x_2}\left[\vartheta_t\left(\frac{\partial}{\partial x_2}(u_1) + \frac{\partial}{\partial x_1}(u_2)\right)\right] \tag{51}$$

$$\frac{\partial}{\partial t}(u_1) + \frac{\partial}{\partial x_3}(u_1 u_3) = -\frac{\partial}{\partial x_1}\left(\frac{p}{\rho} + \frac{2}{3}k\right) + \frac{\partial}{\partial x_3}\left[\vartheta_t\left(\frac{\partial}{\partial x_3}(u_1) + \frac{\partial}{\partial x_1}(u_3)\right)\right] \tag{52}$$

$$\frac{\partial}{\partial t}(u_2) + \frac{\partial}{\partial x_1}(u_2 u_1) = -\frac{\partial}{\partial x_2}\left(\frac{p}{\rho} + \frac{2}{3}k\right) + \frac{\partial}{\partial x_1}\left[\vartheta_t\left(\frac{\partial}{\partial x_1}(u_2) + \frac{\partial}{\partial x_2}(u_1)\right)\right] \tag{53}$$

$$\frac{\partial}{\partial t}(u_2) + \frac{\partial}{\partial x_2}(u_2 u_2) = -\frac{\partial}{\partial x_2}\left(\frac{p}{\rho} + \frac{2}{3}k\right) + \frac{\partial}{\partial x_2}\left[\vartheta_t\left(\frac{\partial}{\partial x_2}(u_2) + \frac{\partial}{\partial x_2}(u_2)\right)\right] \tag{54}$$

$$\frac{\partial}{\partial t}(u_2) + \frac{\partial}{\partial x_3}(u_2 u_3) = -\frac{\partial}{\partial x_2}\left(\frac{p}{\rho} + \frac{2}{3}k\right) + \frac{\partial}{\partial x_3}\left[\vartheta_t\left(\frac{\partial}{\partial x_3}(u_2) + \frac{\partial}{\partial x_2}(u_3)\right)\right] \tag{55}$$

$$\frac{\partial}{\partial t}(u_3) + \frac{\partial}{\partial x_1}(u_3 u_1) = -\frac{\partial}{\partial x_3}\left(\frac{p}{\rho} + \frac{2}{3}k\right) + \frac{\partial}{\partial x_1}\left[\vartheta_t\left(\frac{\partial}{\partial x_1}(u_3) + \frac{\partial}{\partial x_3}(u_1)\right)\right] \tag{56}$$

$$\frac{\partial}{\partial t}(u_3) + \frac{\partial}{\partial x_2}(u_3 u_2) = -\frac{\partial}{\partial x_3}\left(\frac{p}{\rho} + \frac{2}{3}k\right) + \frac{\partial}{\partial x_2}\left[\vartheta_t\left(\frac{\partial}{\partial x_2}(u_3) + \frac{\partial}{\partial x_3}(u_2)\right)\right] \tag{57}$$

$$\frac{\partial}{\partial t}(u_3) + \frac{\partial}{\partial x_3}(u_3 u_3) = -\frac{\partial}{\partial x_3}\left(\frac{p}{\rho} + \frac{2}{3}k\right) + \frac{\partial}{\partial x_3}\left[\vartheta_t\left(\frac{\partial}{\partial x_3}(u_3) + \frac{\partial}{\partial x_3}(u_3)\right)\right] \tag{58}$$

4.1.3 TRANSPORT EQUATION FOR k:

$$\frac{\partial}{\partial t}(k) + \frac{\partial}{\partial x_1}(k u_1) = \frac{\partial}{\partial x_1}\left(\frac{\vartheta_t}{\sigma_1}\frac{\partial}{\partial x_1}k\right) + \vartheta_t s - \varepsilon \tag{59}$$

$$\frac{\partial}{\partial t}(k) + \frac{\partial}{\partial x_2}(k u_2) = \frac{\partial}{\partial x_2}\left(\frac{\vartheta_t}{\sigma_1}\frac{\partial}{\partial x_2}k\right) + \vartheta_t s - \varepsilon \tag{60}$$

$$\frac{\partial}{\partial t}(k) + \frac{\partial}{\partial x_3}(k u_3) = \frac{\partial}{\partial x_3}\left(\frac{\vartheta_t}{\sigma_1}\frac{\partial}{\partial x_3}k\right) + \vartheta_t s - \varepsilon \tag{61}$$

4.1.4 TRANSPORT EQUATION FOR ε

$$\frac{\partial}{\partial t}(\varepsilon) + \frac{\partial}{\partial x_1}(\varepsilon u_1) = \frac{\partial}{\partial x_1}\left(\frac{\vartheta_t}{\sigma_2}\frac{\partial}{\partial x_1}\varepsilon\right) + C_1\frac{\varepsilon}{k}\vartheta_t s - C_2\frac{\varepsilon^2}{k} \tag{62}$$

$$\frac{\partial}{\partial t}(\varepsilon) + \frac{\partial}{\partial x_2}(\varepsilon u_2) = \frac{\partial}{\partial x_2}\left(\frac{\vartheta_t}{\sigma_2}\frac{\partial}{\partial x_2}\varepsilon\right) + C_1\frac{\varepsilon}{k}\vartheta_t s - C_2\frac{\varepsilon^2}{k} \tag{63}$$

$$\frac{\partial}{\partial t}(\varepsilon) + \frac{\partial}{\partial x_3}(\varepsilon u_3) = \frac{\partial}{\partial x_3}\left(\frac{\vartheta_t}{\sigma_2}\frac{\partial}{\partial x_3}\varepsilon\right) + C_1\frac{\varepsilon}{k}\vartheta_t s - C_2\frac{\varepsilon^2}{k} \tag{64}$$

$$\vartheta_t = k^{0.5} l = C_0 k^2 / \varepsilon$$

$$\sigma_1 = 1.0 \qquad C_0 = 0.09$$
$$\sigma_2 = 1.3 \qquad C_1 = 1.44$$
$$C_2 = 1.92$$

$$s = \left(\frac{\partial}{\partial x_j}(u_i) + \frac{\partial}{\partial x_i}(u_j) \right) \frac{\partial}{\partial x_j}(u_i)$$ (65)

4.2 BOUNDARY CONDITIONS

The equations described in the above section are solved to predict the air velocity and temperature distribution in mechanically ventilated (heated or cooled) rooms. Since the boundary conditions are unique to a particular flow situation, an accurate representation of these conditions is necessary for a reliable solution to be achieved. For the ventilated rooms it is necessary to specify the conditions as inlet, outlet and on the internal surfaces of the room. In general three types of boundary conditions are used.

4.2.1 INLET CONDITION:

Uniform distribution is used over the inlet boundary of the longitudinal velocity, u_o, temperature, T, kinetic energy of turbulence, k, and the energy dissipation rate, ε. Other quantities such as pressure and the other two velocity components are taken as zero at the inlet.

The kinetic energy of turbulence is calculated using

$$k = (3/2) \, I^2 u_o^2$$ (66)

Where I^2 is the turbulence intensity of the u-component of velocity at the inlet which is taken as 0.14 in the absence of measured values,

The dissipation rate is obtained from

$$\varepsilon = k^{1.5} / (\lambda H)$$ (67)

Where λ is a constant taken as 0.005 and H is the room height or the square root of the cross sectional area of the room.

4.2.2 OUTLET CONDITIONS:

The longitudinal component of velocity u_e is derived from the continuity equation, i.e

$$u_e = u_o \frac{A_o}{A_e} \frac{\rho_o}{\rho_e}$$

(68)

and the other velocity components and the pressure are assumed to be zero. The exit temperature T_e is obtained from the energy equation for the whole flow field taking into account heat transfer across all boundaries. Boundary conditions for k and ε are not required because an up-wind computational scheme, is used expect that their gradients in the exit plane are zero. Uniform distribution of u_e and T_e is assumed across the exit area.

4.2.3 WALL BOUNDARY:

Close to a wall region laminar viscosity becomes more significant than turbulent viscosity as a result of the damping effect of the wall, i.e $\frac{\partial}{\partial y}(k) = 0$ at the wall. So the turbulence model equations do not apply to regions close to a solid boundary and instead the wall-function equations due to launder and spalding are used for the velocity component parallel to the boundary. With in the laminar sublayer region viscous effects pre-dominate and the wall shear stress, τ_w, is described by the usual couette flow expression. At a point outside this region turbulent shear becomes siginificant and it can be shown that when the generation and dissipation of energy is in balance then $\frac{\tau}{\rho} = C_\mu^{0.5} k$

The boundary temperatures can be specified to represent the actual temperatures of the room surfaces or to represent the temperature of a heat source or a sink of a known capacity. Heat fluxes or sinks can be treated as additional source terms in the energy equation [16].

The commercial package CFD code PHOENICS is used to simulate the model equations. Simulations are performed on Intel(R), Pentium(R)D CPU 2.66GHz, 512 MB of RAM based computer.

5.1 DEVELOPMENT OF GEOMETRIC MODEL

Geometrical model (or physical model) has been developed using PHOENICS as follows. Two connecting rooms are modeled with dimensions 10 m length, 5m width and 4m height. Partition is at middle (X=5m). One room is control panel room, where the process control is carried and the second one is rest room.

Control panel room: - An inlet is given as side to face as square shape with 0.75m. The outlet is on the opposite side face as square shape with 0.75m. Both are at a height (or distance) 2.5m from the bottom of the room. One door is given as entrance to control panel room, connected to rest room with rectangular shape of 1.5m width and 2m height. Contaminant is entering as a point source at the bottom position (0, 1.5, 0) with temperature of 50^0C.

Rest room: - for rest room, the outlet of control panel becomes inlet. Other outlet is in opposite side to face of inlet with square shape of 0.75m is given. Two doors are given in rectangular shape with 2m height and 1.5m width in which one is the entrance for rest room and other is entrance for control panel room.

5.2 BOUNDARY CONDITIONS AND FLOW PROPERTIES

Boundary conditions used for the flow variables in the simulation as listed in

Table 1:

Variable	Wall	Inlet	Outlet
u	0	0	outflow
v	0	0.1 m/s at X=0m, Y=2.755m to Y=3.505m, Z=2.5m to Z=3.25m	outflow
w	0	0	outflow
C	0	0.01 m/s at X=0m, Y=1.5m, Z=0m	Outflow
k	k-equation	TI=5%,L=0.01 m	zero gradient
e	wall-function	TI=5%,L=0.01 m	zero gradient

TI is turbulent intensity and L is a characteristic length.

In numerical simulations, fluid properties are held constant with value corresponding to a room temperature of $22^{0}C$. The air density is 1.189 kg/m^3 and viscosity is $1.72*10^{-4}$ kg/m s

As contaminant is coming from industry it will contain density more than air. In this case contaminant is twice the air density.

Theory:-

The density is to be calculated using the mass fraction in each cell, hence,

$$1/\rho = 1 / (C_1/\rho_1 + C_2/\rho_2) \tag{69}$$

where, ρ_1 is the density of the contaminant (2 x 1.189 kg/m^3), ρ_2 is the density of air (1.189 kg/m^3), C_1 is the mass fraction of contaminant and C_2 is the mass fraction of air (actually 1-C_1).

One of the available density relationships is 'Inverse linear'. This uses the following expression for density:

$$\rho = 1/ (A + B\ \phi) \tag{70}$$

where r is the resulting density in each cell and f is the variable.

Manipulating expression (69) to be in the same form as expression (70),

$$\rho = 1/ ((1/\rho_2) + (\rho_2 - \rho_1) / (\rho_1\ \rho_2)\ C_1)$$

Hence, $A = 1/\rho_2$; $B = (\rho_2 - \rho_1) / (\rho_1\ \rho_2)$; $\phi = C_1$

36

5.3 NUMERICAL SOLUTION PROCEDURE

In PHOENICS, the continuous governing equations are converted into finite difference equations via integration over control volumes created by a uniform rectangular grid of $30 \times 30 \times 30$ size. The power law scheme is used to discretize the convective terms in space. Formally, this scheme exhibits first-order accuracy when the cell Reynolds number is low and second-order accuracy when the cell Reynolds number is high. The diffusion terms are discretized by finite differencing. This differencing is second-order accurate.

The discrete equations are solved under the imposed boundary conditions with an iterative procedure that implements the Line Gauss–Seidel method and the SIMPLE algorithm.

At air inlet, air velocity is 0.1m/s with Re=519. The difficulty with this velocity is that the inlet contains a disturbed laminar flow. The inlet section is not long enough for the boundary layers to converge, so the majority of the inlet air velocity profile is that of laminar plug flow. The low flow velocity makes the system inherently more sensitive to small disturbances and thermal gradients in the numerical simulation.

5.4 DEVELPOMENT OF GEOMETRIC MODEL ON PHOENICS

Accessing PHOENICS-VR

From the system level:

To enter the PHOENICS-VR environment, click on the PHOENICS icon on the desktop, or click on Start, programs, PHOENICS, PHOENICS.

In PHOENICS-VR environment,

Start with an 'empty' case - click on 'File' then on 'Start New Case', then on 'Core', then click on 'OK'; to confirm the resetting.

To enter VR Editor:

This is the default mode of operation.

Within VR Editor

Set the domain size and activate solution of the required variables:

Click on 'main menu' and then on 'geometry'.

Change X-domain size as 10m

Change Y-domain size as 5m

Change Z-domain size as 4m

Click on 'Models'

Set the 'solution for velocity and pressure' ON

Energy equation 'Temperature'.

Click on 'static' change to 'TOTAL'

Select 'Turbulence models' laminar

Click on 'previous panel'

Click on 'TOP MENU' and 'OK'

5.4.1 Creation of partition having door and one outlet between control panel room and rest room.

Create Object B1

Click on 'NEW OBJECT'

Type : Plate

Set position and size as

X_{pos} : 5.0 X_{size} : 0.0

Y_{pos} : 2.0 Y_{size} : 3.0

Z_{pos} : 0.0 Z_{size} : 2.5

Click on 'OK' to close object dialogue box.

Create Object B2

Click on 'NEW OBJECT'

Type : Plate

Set position and size as

X_{pos} : 5.0 X_{size} : 0.0

Y_{pos} : 0.0 Y_{size} : 0.5

Z_{pos} : 0.0 Z_{size} : 2.5

Click on 'OK' to close object dialogue box.

Create Object B3 for door

Click on 'NEW OBJECT'

Type : inlet

Set position and size as

X_{pos} : 5.0 X_{size} : 0.0

Y_{pos} : 0.5 Y_{size} : 1.5

Z_{pos} : 0.0 Z_{size} : 2.0

Click on 'OK' to close object dialogue box.

Create Object B4

Click on 'NEW OBJECT'

Type : Plate

Set position and size as

X_{pos} : 5.0 X_{size} : 0.0

Y_{pos} : 0.5 Y_{size} : 1.5

Z_{pos} : 2.0 Z_{size} : 0.5

Click on 'OK' to close object dialogue box.

Create Object B17

Click on 'NEW OBJECT'

Type : outlet

Set position and size as

X_{pos} : 5.0 X_{size} : 0.0

Y_{pos} : 2.75 Y_{size} : 0.75

Z_{pos} : 2.5 Z_{size} : 0.75

Click on 'OK' to close object dialogue box.

Create Object B18

Click on 'NEW OBJECT'

Type : Plate

Set position and size as

X_{pos} : 5.0 X_{size} : 0.0

Y_{pos} : 3.5 Y_{size} : 1.495

Z_{pos} : 2.5 Z_{size} : 0.752

Click on 'OK' to close object dialogue box.

Create Object B19

Click on 'NEW OBJECT'

Type : Plate

Set position and size as

X_{pos} : 5.0 X_{size} : 0.0

Y_{pos} : 0.0 Y_{size} : 5.0

Z_{pos} : 3.248 Z_{size} : 0.75

Click on 'OK' to close object dialogue box.

Create Object B20

Click on 'NEW OBJECT'

Type : Plate

Set position and size as

X_{pos} : 5.0 X_{size} : 0.0

Y_{pos} : 0.0 Y_{size} : 2.755

Z_{pos} : 2.5 Z_{size} : 0.752

Click on 'OK' to close object dialogue box.

5.4.2 Creation of wall at the end of rest room having door and one outlet (X=10m)

Create object B9

Select B1

Click on 'Duplicate object or group' button on the handset

Click on 'X position up' until the duplicate object has moved to last (X=10)

Create object B10

Select B18

Click on 'Duplicate object or group' button on the handset

Click on 'X position up' until the duplicate object has moved to last (X=10)

Create object B11

Select B19

Click on 'Duplicate object or group' button on the handset

Click on 'X position up' until the duplicate object has moved to last (X=10)

Create object B12

Select B17

Click on 'Duplicate object or group' button on the handset

Click on 'X position up' until the duplicate object has moved to last (X=10)

Create object B13

Select B20

Click on 'Duplicate object or group' button on the handset

Click on 'X position up' until the duplicate object has moved to last (X=10)

Create object B14

Select B3

Click on 'Duplicate object or group' button on the handset

Click on 'X position up' until the duplicate object has moved to last (X=10)

Create object B15

Select B4

Click on 'Duplicate object or group' button on the handset

Click on 'X position up' until the duplicate object has moved to last (X=10)

Create object B16

Select B2

Click on 'Duplicate object or group' button on the handset

Click on 'X position up' until the duplicate object has moved to last (X=10)

5.4.3 Creation of all at the beginning having one inlet (X=0)

Create object B5

Select B17

Click on 'Duplicate object or group' button on the handset

Click on 'X position down' until the duplicate object has moved to first (X=0)

Click on 'attribute'

Change velocity to 0.1 m/s

Click on 'general'

Type : inlet

Create object B6

Select B19

Click on 'Duplicate object or group' button on the handset

Click on 'X position down' until the duplicate object has moved to first (X=0)

Create object B7

Select B18

Click on 'Duplicate object or group' button on the handset

Click on 'X position down' until the duplicate object has moved to first (X=0)

Create object B8

Select B2

Click on 'Duplicate object or group' button on the handset

Click on 'X position down' until the duplicate object has moved to first (X=0)

Create object B21

Click on 'new object'

Type : plate

Set position and size as

X_{pos} : 0.0 X_{size} : 0.0

Y_{pos} : 0.0 Y_{size} : 5.0

Z_{pos} : 0.0 Z_{size} : 2.5

Click on 'OK' to close object dialogue box.

Create object ground

Click on 'new object'

Type : plate

Name : ground

Set position and size as

X_{pos} : 0.0 X_{size} : 10.0

Y_{pos} : 0.0 Y_{size} : 5.0

Z_{pos} : 0.0 Z_{size} : 0.0

Click on 'OK' to close object dialogue box

Create object B23

Select ground

Click on 'Duplicate object or group' button on the handset

Click on 'Z position up' until the duplicate object has moved to first (Z=4)

Create object B24

Click on 'new object'

Type : plate

Set position and size as

X_{pos} : 0.0 X_{size} : 10.0

Y_{pos} : 5.0 Y_{size} : 0.0

Z_{pos} : 0.0 Z_{size} : 4.0

Click on 'OK' to close object dialogue box

Create object B25

Select B24

Click on 'Duplicate object or group' button on the handset

Click on 'Y position up' until the duplicate object has moved to first (Y=0)

5.4.4 Creation of contaminant Source

Click on 'main menu'

Click on 'models'

Click on 'solution controls/extra variables'

In SOLVE entry box, type C1 and click on apply.

Click on the > button next to variable, and new variable called C1 is apprears. This will represent the mass fraction of contaminant.

Create object for contaminant flow

Click on 'new object'

Type : inlet

Name : contaminant

Set position and size as

X_{pos} : 0.0 X_{size} : 0.0

Y_{pos} : 1.5 Y_{size} : 0.1

Z_{pos} : 0.0 Z_{size} : 0.1

Click on 'OK' to close object dialogue box

Click on 'attributes'

Change velocity to 0.01m/s

Change temperature 50°C.

Set the grid:

Click on the 'Mesh toggle' button. The default mesh (shown as orange lines) will appear on the screen.

Right click anywhere on the image, and the 'Grid mesh settings' dialog box will appear. Change the Number of cells to 30 cells in X, 30 cells in Y and 30 cells in Z. Click on 'OK'; to close the dialog box. The mesh will now be shown as blue and orange lines. The orange lines are 'regions', defined by the bounding boxes of the objects. Click on 'Mesh toggle' again to turn off the mesh display.

Set the remaining solution-control parameters:

Click on 'Main Menu' and then on 'Numerics'.

Set the number of iterations to

Click on 'Top menu' to return to the top menu.

Click on 'OK' to exit the Main Menu.

Running the Solver.

In the PHOENICS-VR environment, click on 'Run', 'Solver'(Earth), and click on 'OK'; to confirm running Earth.

Using the VR Viewer

In the PHOENICS-VR environment, click on 'Run', 'Post processor', then GUI Post processor (VR Viewer). Click 'OK' on the file names dialog to accept the default files.

To view:

- Vectors - click on the 'Vector toggle'
- Contours - click on the 'Contour toggle'
- Streamlines - click on the 'Create Streamline' button
- Iso-surfaces - click on the 'Iso-Surface toggle'

To select the plotting variable:

- To select Pressure - click on the 'Select Pressure button' P .
- To select Velocity - click on the 'Select Velocity button'
- To select Temperature - click on the 'Select Temperature button'
- To select any other variable - click on the 'Select a Variable button' C. Select DEN1 for density, or ENUL for laminar viscosity values.

To change the direction of the plotting plane, set the slice direction to X, Y or Z

To change the position of the plotting plane, move the probe using the probe position buttons

A typical plot from this case is:
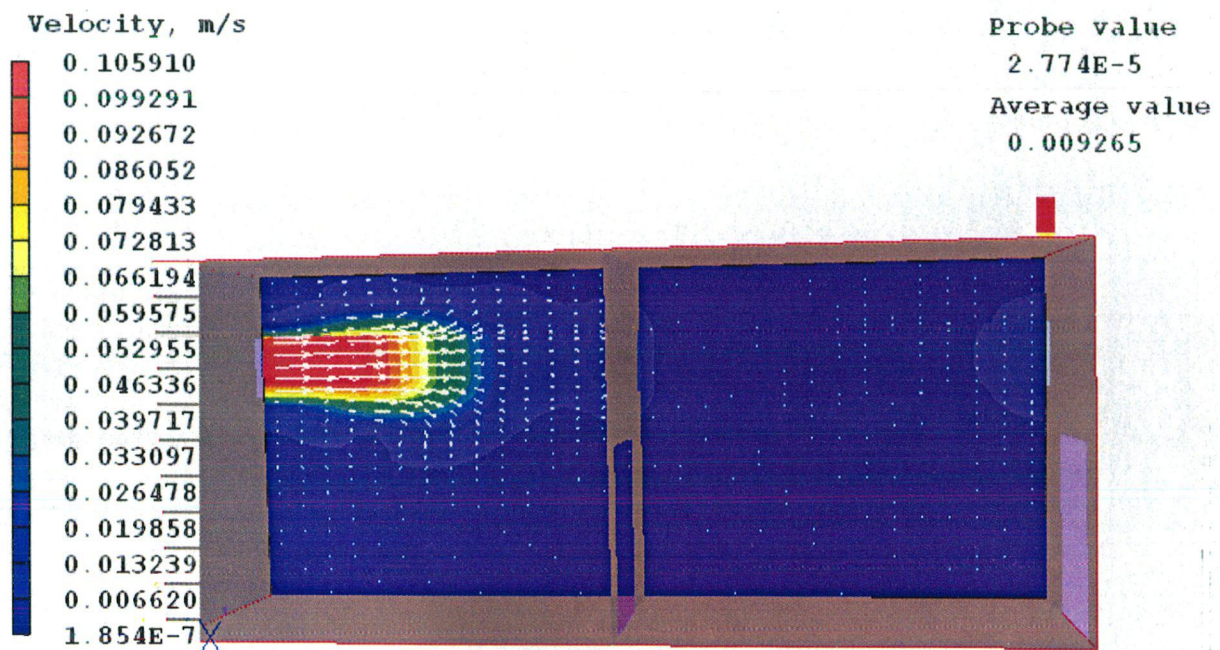
Fig.2 Velocity profile at inlet

Saving the results

In the PHOENICS-VR environment, click on 'Save as a case', make a new folder called 'control panel ' (e.g.) and save as 'CASE1' (e.g.).

6.1 SOLUTION INITIALIZATION AND ITERATION

Solution initialization and iteration are carried out till the solution gets converged on convergence criteria ± 0.0001. Two different representation of the fluid flow in the room are used: laminar flow, turbulent flow using the standard k-ε turbulence model. The governing equations for the indoor air system are the mass conservation equation and the Navier-Stokes equations as described in chapter 4.

For laminar simulation:-

Min	Max	Spot Value	Change	Variable	Max	% Error	Change
-6.00E+00	1.00E+00	3.15E-04	-3.47E-07	P1	2.00E+07	1.68E+01	-4.03E-02
0.00E+00	4.00E-03	9.41E-04	-2.66E-06	U1	3.98E+09	4.08E+05	-2.18E+02
-2.00E-01	1.00E-01	-2.18E-04	-3.80E-09	V1	1.00E+08	1.01E+06	7.09E+01
-7.00E-04	3.00E-04	-4.55E-04	-5.59E-08	W1	1.00E+15	9.65E+05	1.31E+02
0.00E+00	1.00E-02	8.57E-03	-2.84E-06	C1	2.00E+05	8.73E+03	-8.63E+01
-3.00E+02	1.00E+02	3.88E-01	-6.83E-04	TEM1	1.00E+11	3.70E+00	-4.94E-03

NX	NY	NZ	ISWEEP	967	Time now	13:29
30	30	30	IZSTEP OFF		(m:s) est	13:30

Press a character key to interrupt.

Fig.3 Convergence for laminar model

From fig.3, for laminar model number of iterations for convergence is 967 and time taken for convergence is 13 minute 29 second.

For standard k-ε simulation:-

Min	Max	Spot Value	Change	Variable	Max	% Error	Change
-6.00E+00	1.00E+00	3.24E-04	-3.07E-07	P1	2.00E+07	1.58E+01	-3.75E-02
0.00E+00	4.00E-03	9.53E-04	-2.59E-06	U1	3.98E+09	3.87E+05	-2.70E+02
-2.00E-01	1.00E-01	-2.23E-04	-1.35E-08	V1	1.00E+08	9.63E+05	-4.69E+01
-7.00E-04	2.00E-04	-4.63E-04	-6.84E-08	W1	1.00E+15	9.26E+05	4.31E+01
0.00E+00	3.00E-06	2.32E-06	5.19E-09	kE	3.16E+06	2.38E+04	-8.04E+00
0.00E+00	4.00E-09	3.22E-09	8.10E-12	EP	2.00E+07	2.32E+04	-8.19E+00
0.00E+00	2.00E-02	6.28E-03	-2.16E-05	C1	1.58E+05	1.58E+04	-7.72E+01
-3.00E+02	1.00E+02	2.91E-01	-9.25E-04	TEM1	1.00E+11	2.63E+00	-1.57E-03

NX	NY	NZ	ISWEEP	967	Time	now	18:56
30	30	30	IZSTEP	OFF	(m:s)	est	18:57

Fig.4 Convergence for k-ε model

From fig.4, k-ε model number of iterations for convergence is 967 same as laminar model with simulation time 18 minute 56 second.

Therefore k-ε model is more expensive than laminar model.

6.2 PROFILES

Vectors and contours of velocity of air, pressure, temperature and contaminant distribution is important. For different surfaces as Y=1m, Y=2m, Y=3m, Y=4m, Y=5m, at different heights as Z=0.5m, Z=1m, Z=2m, Z=3m, Z=4m throughout the length of the room variation in variables are plotted.

6.2.1 Variation/Profiles of Velocity
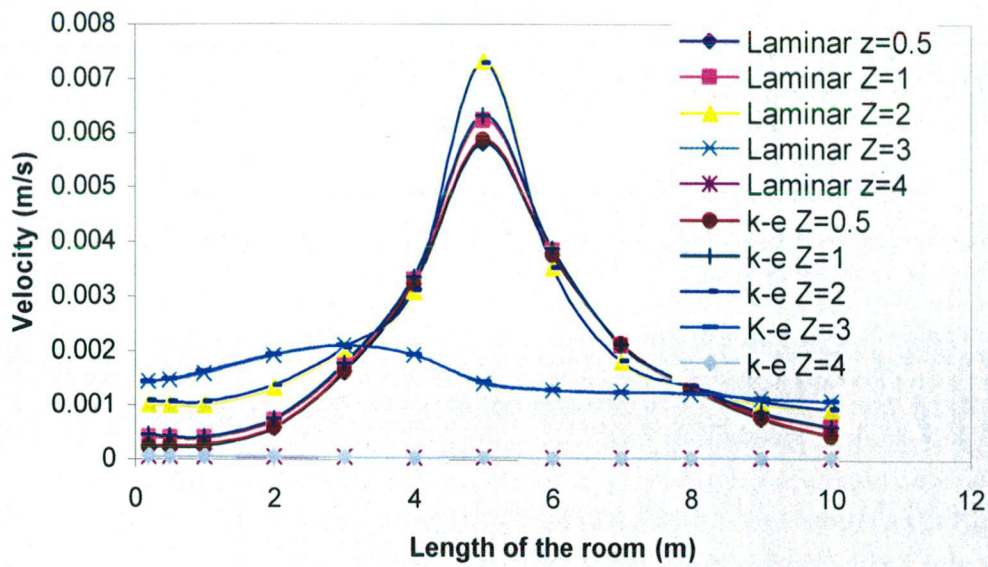
Fig.5 Velocity profile at Y=1m for different heights

From fig.5 velocity is high at the partition of rooms. At heights Z=4m velocity is very low and at Z =3m also velocity is low compare to heights at Z=0.5m, Z=1m, Z =2m. From fig.5 we can see that near to roof velocity is very low. Both laminar and k-ε models are giving same results. Contour plot corresponding to this velocity profiles is in fig.6.
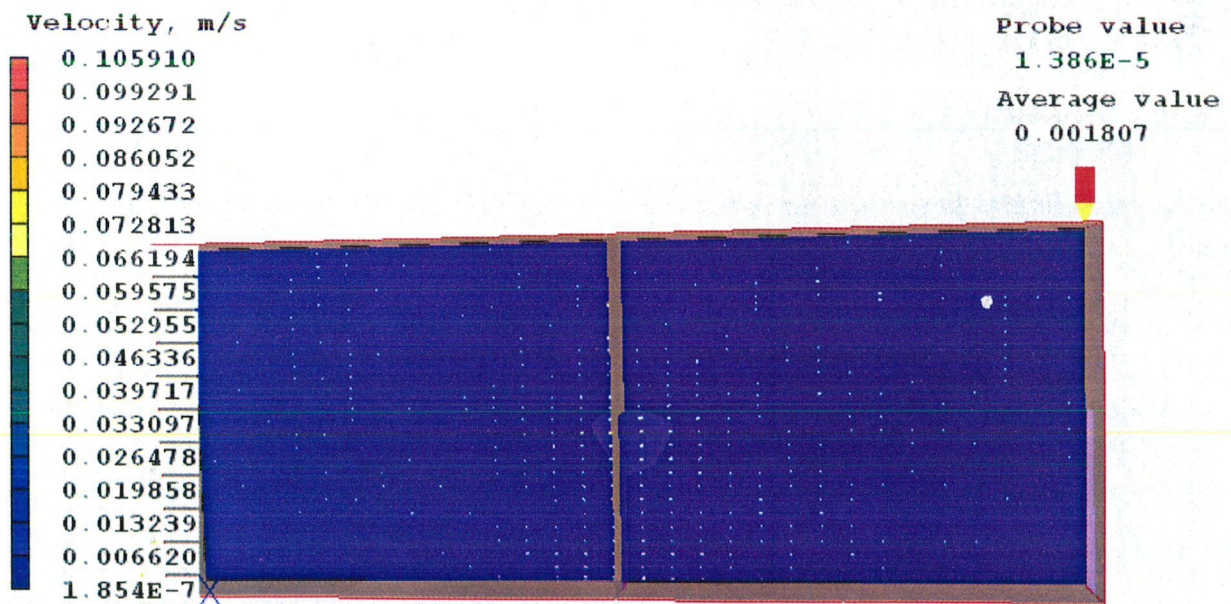
Fig.6 Contour plot of velocity at Y=1m
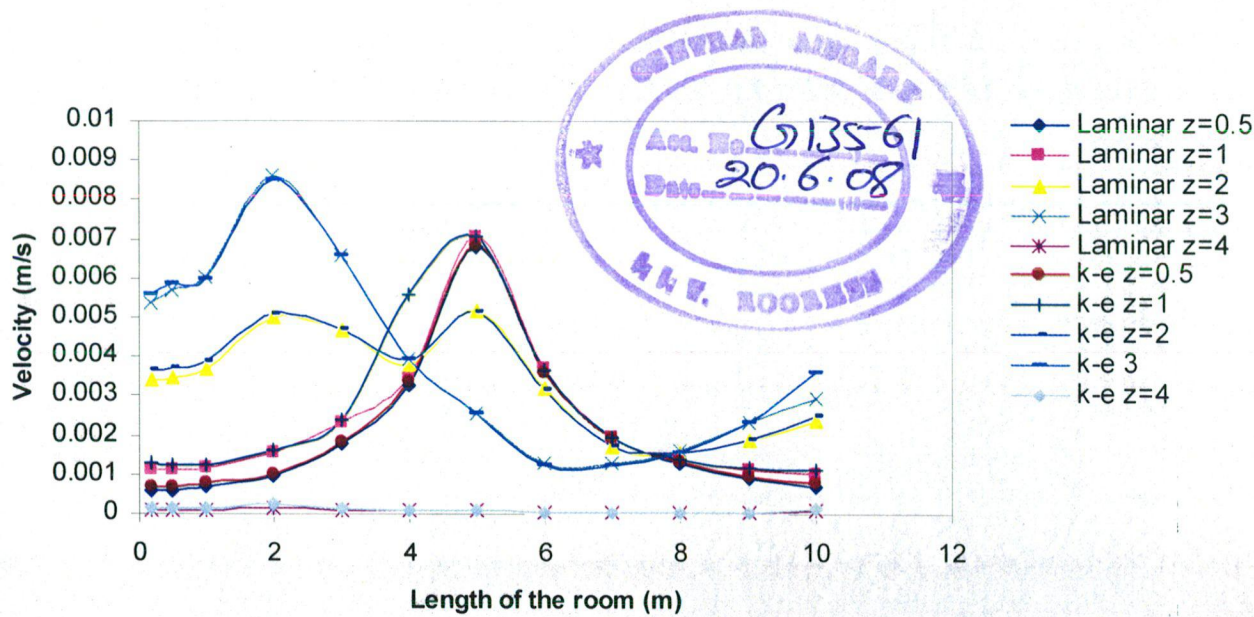
Fig.7 Velocity profile at Y=2m for different heights

From fig.7 velocity at ceiling (Z=4m) is very low. At different heights both laminar and k-ε gives the same result. The contour plot corresponding to this velocity profile is in fig.8.
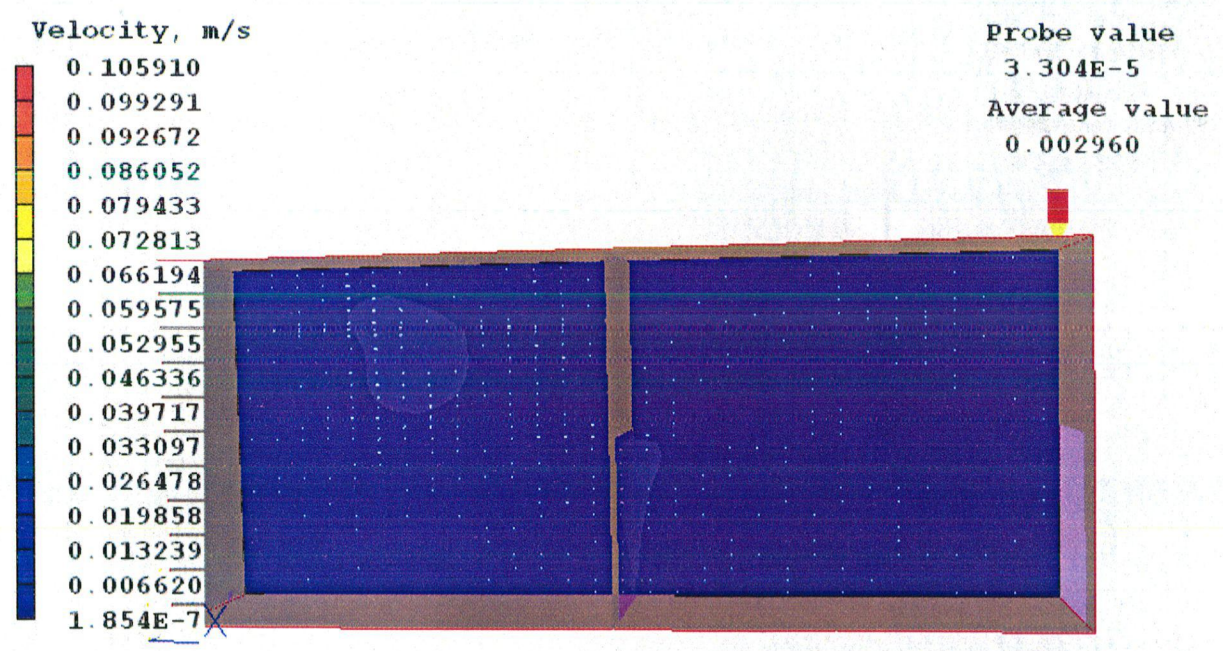
Fig.8 Contour plot of velocity at Y=2m
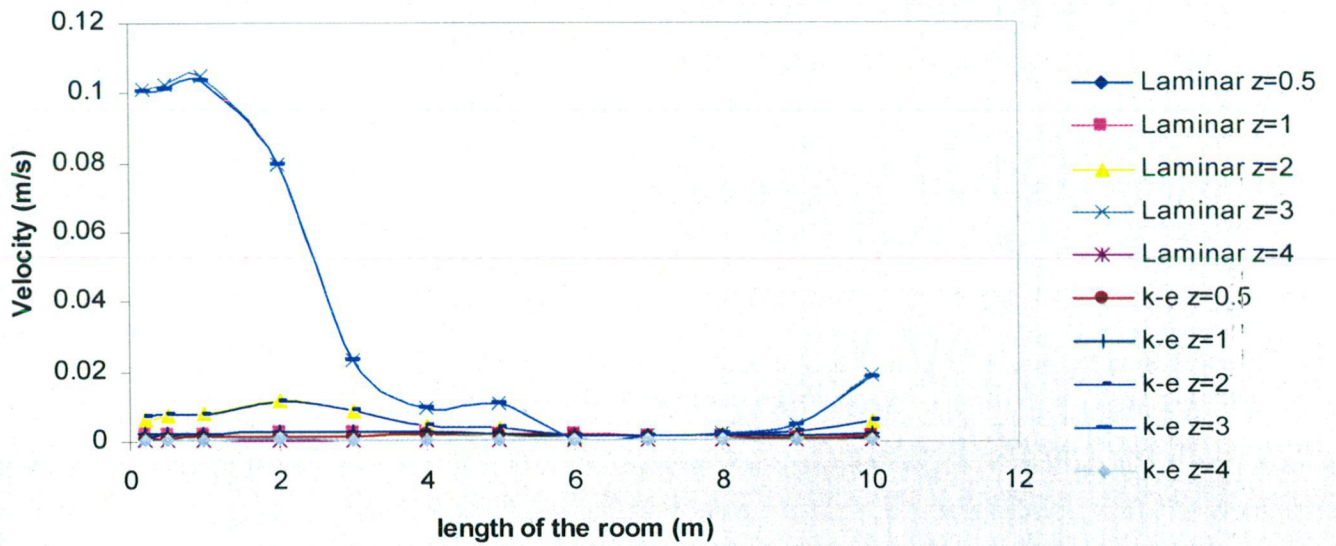
Fig.9 Velocity profile at Y=3m for different heights

From fig.9 velocity at ceiling and at ground is very low. Velocity at Z=3m near the inlet is high and at all remaining heights velocity is low. Both laminar and k-ε gives the same result. The contour plot corresponding to this velocity profile is in fig.10.
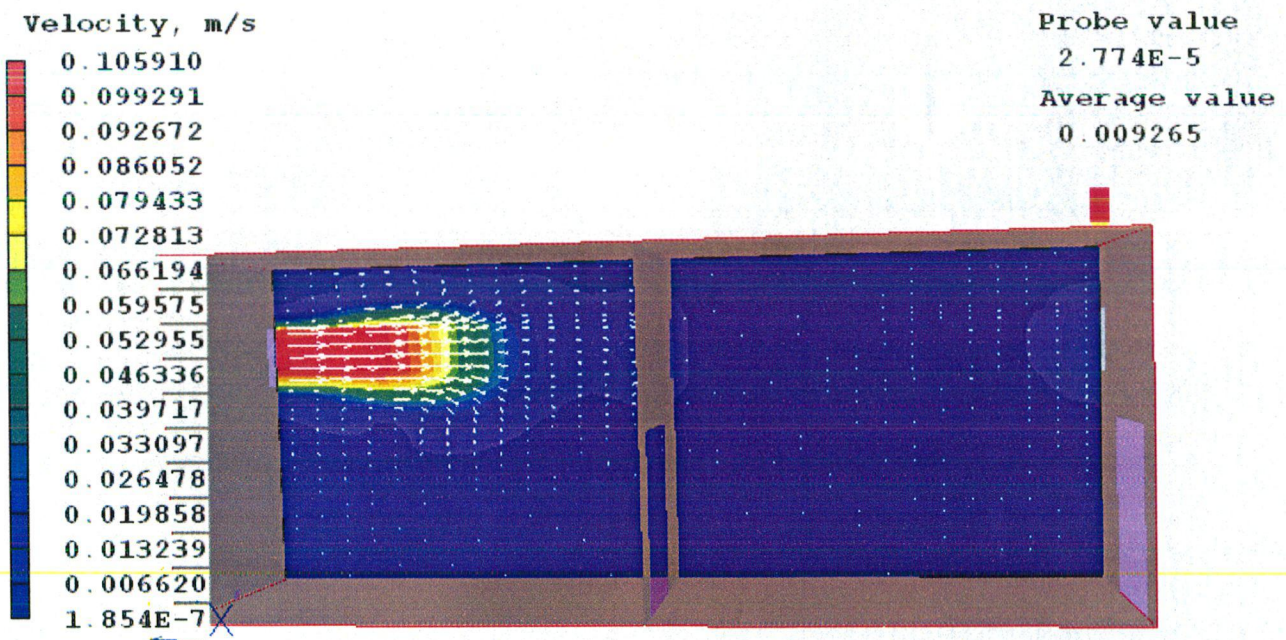
Fig.10 Contour plot of velocity at Y=3m

51
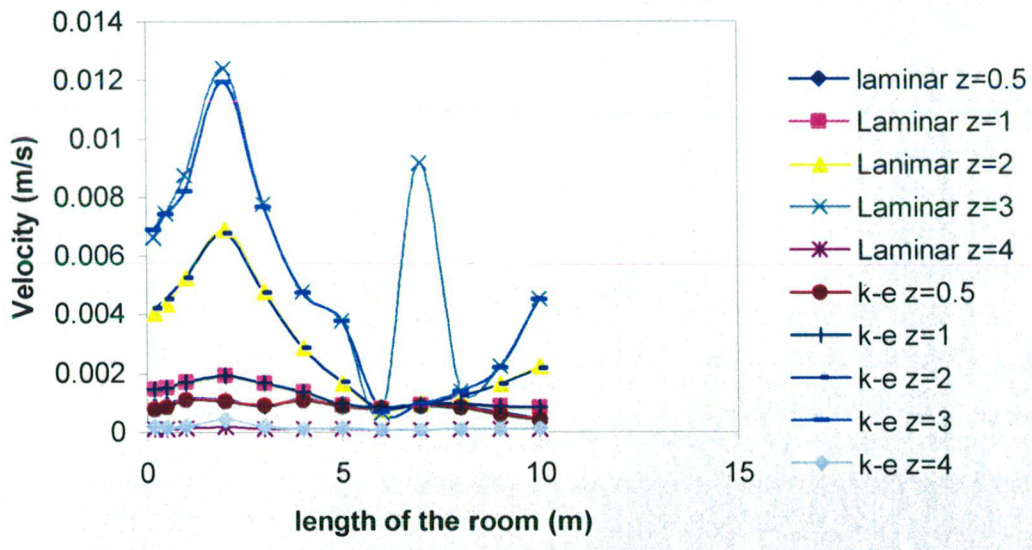
Fig.11 Velocity profile at Y=4m for different heights

From fig.11 at ceiling the velocity is very low. At ground comparing to ceiling it is slightly high, but it is low velocity. Laminar model gives slightly better results than k-ε model. The contour plot corresponding to this velocity profile is in fig.12.
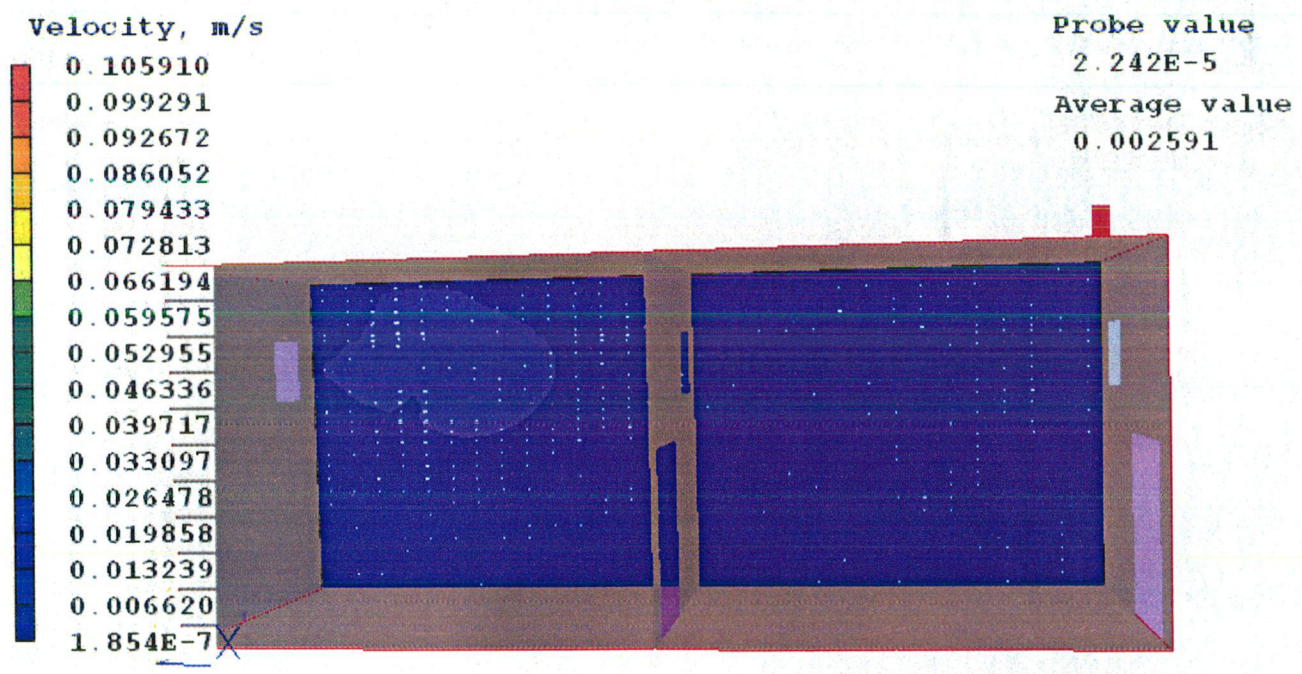
Fig.12 Contour plot of velocity at Y=4m
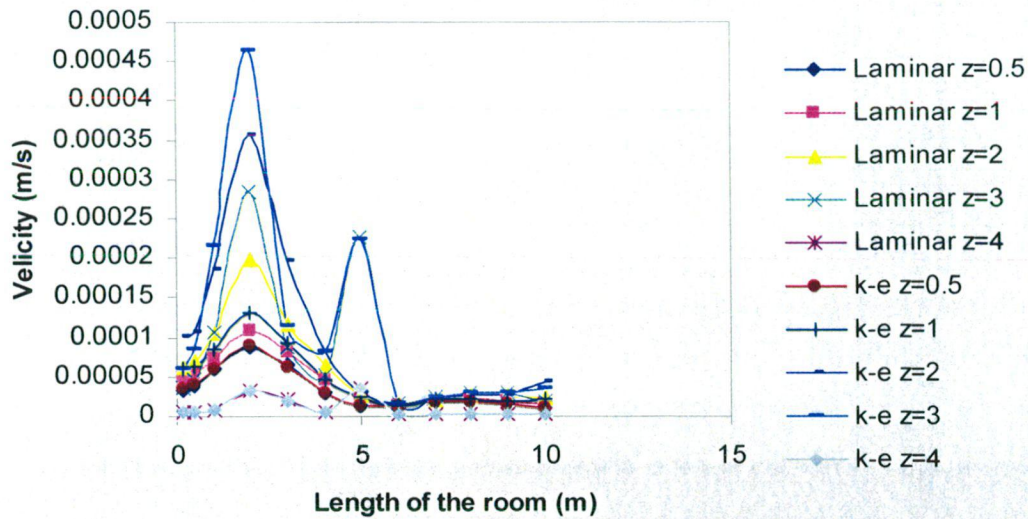
Fig.13 Velocity profile at Y=5m for different heights

From fig.13 near the ceiling (Z=4m) and ground (Z=0.5m) both models gives the same result. But at Z=3m, Z=2m, Z=1m there is lot of variation as it is near to inlet. The contour plot corresponding to this velocity profile is in fig.14.
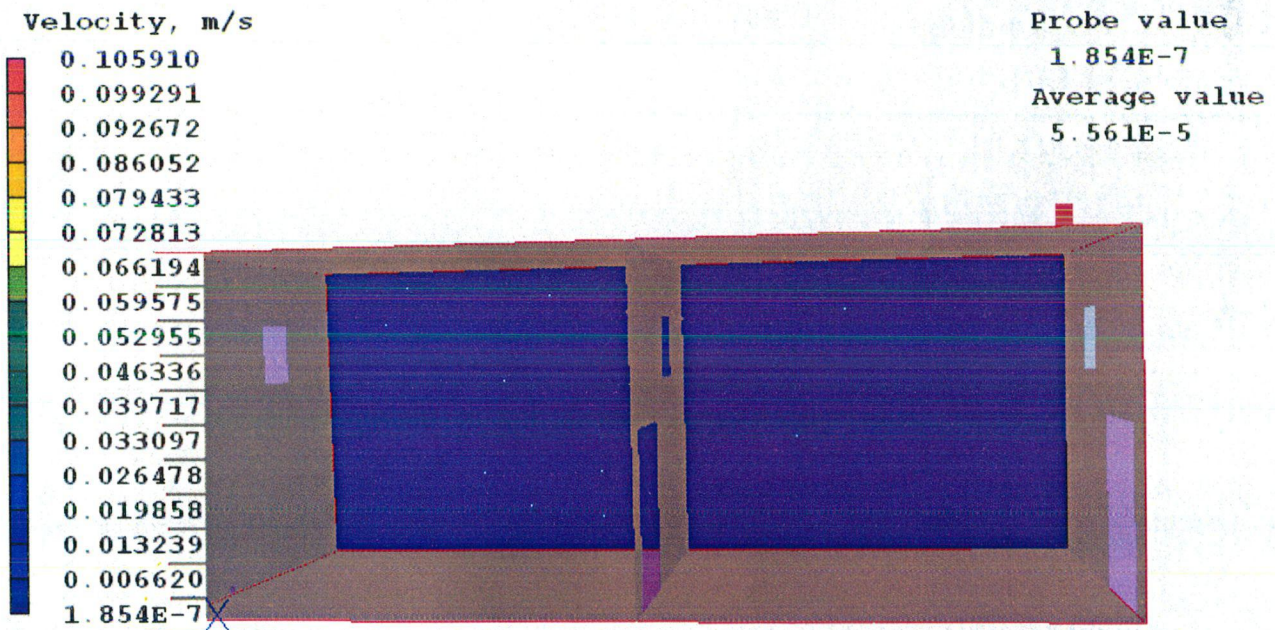
Fig.14 Contour plot of velocity at Y=5m

From velocity plots, it can be shown that the air enter with high velocity. The remaining portion of the air is at low velocity as some air gets recirculated by the turbulent flow. As the air moving away from the inlet, it moves like a jet and gets outward. From velocity plots it can be concluded that the air particles get low

53

velocity as they moving away from inlet. At the edges and corners due to formation of vectors, air velocity will be slightly high than remaining part of the room.

6.2.2 Variation/Profiles of Pressure
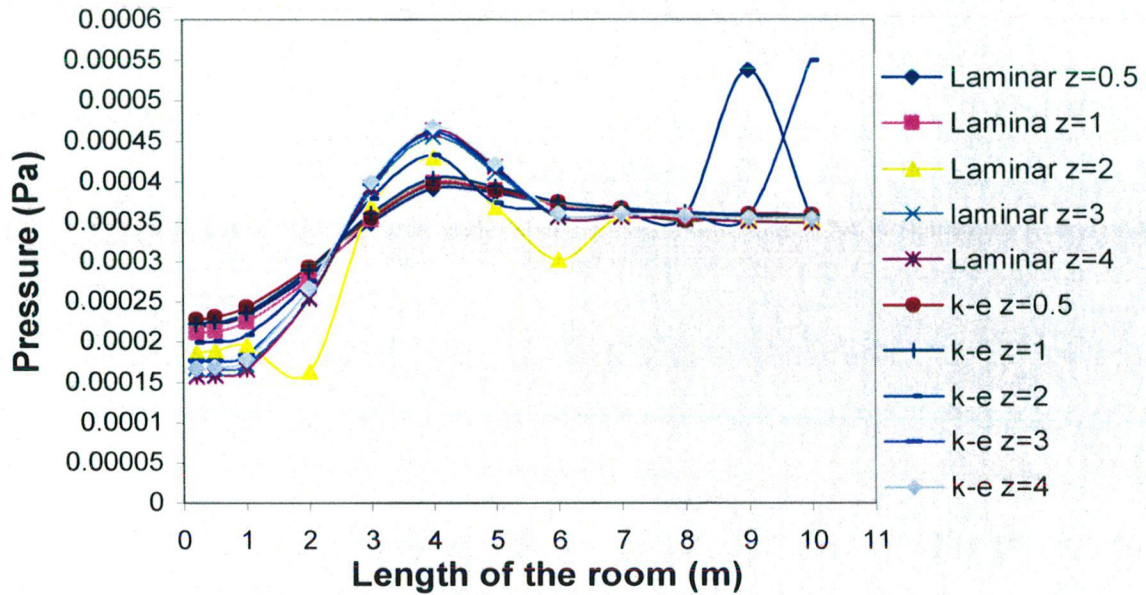
Fig.15 Pressure profile at Y=1m for different heights

From fig.15 there not much difference in pressures at X=0m but as the length increases pressure is increasing and at wall (partition) there is lower in pressure and becomes constant. For Z=0.5m and 2m there is sudden increase and decrease in pressures. Contour plot corresponding to this pressure profile is in fig.16
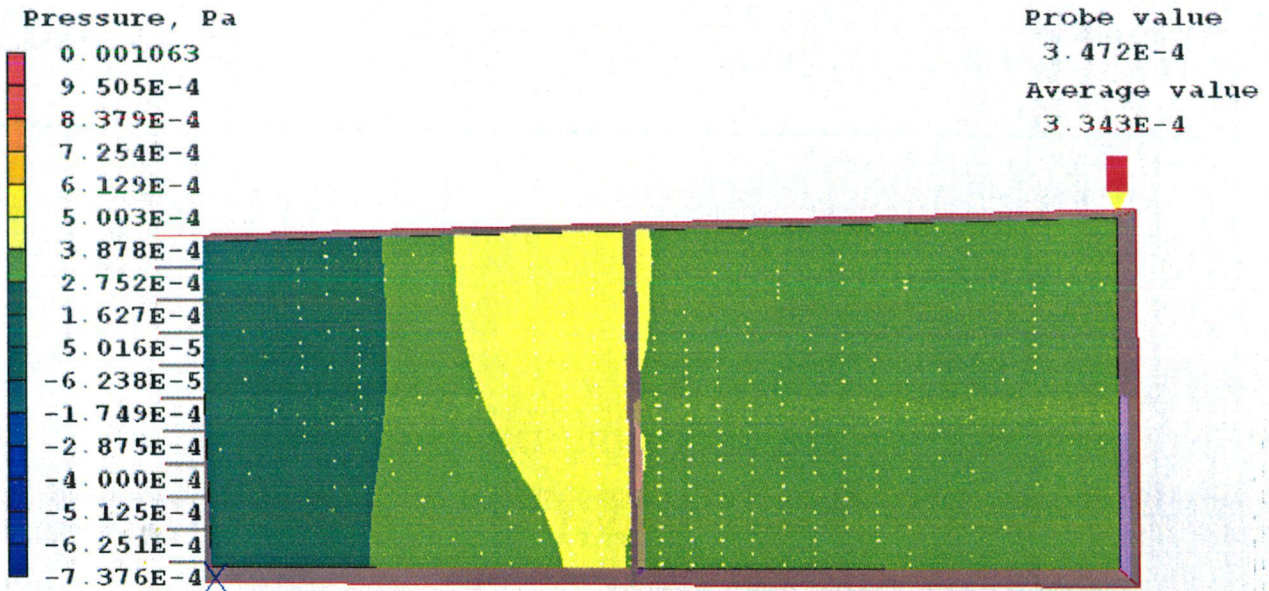
Fig.16 Contour plot of pressure at Y=1m
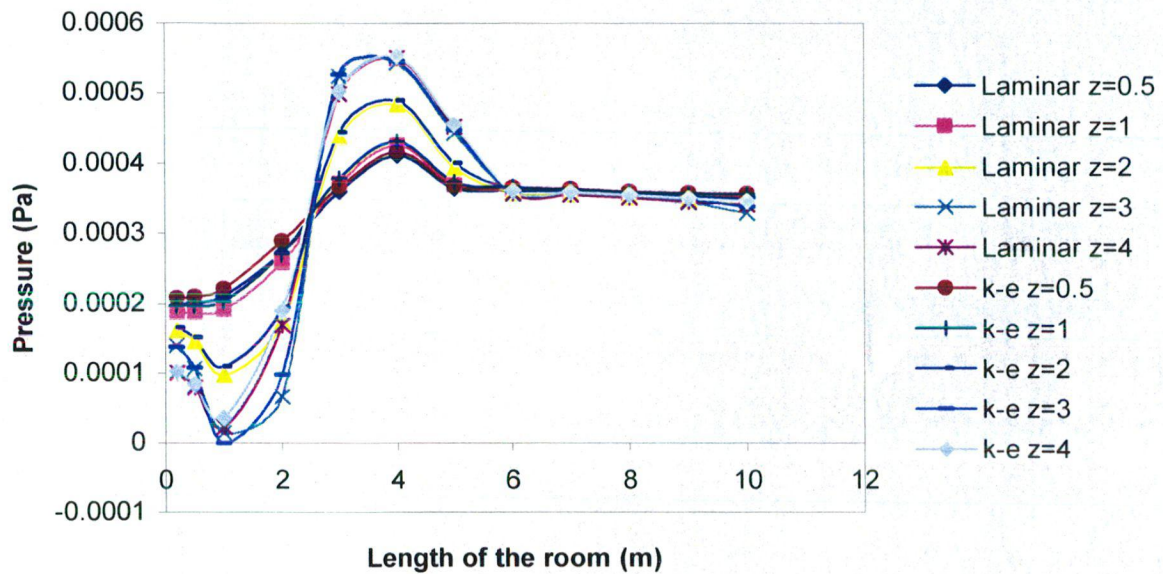
Fig.17 Pressure profile at Y=2m for different heights

From fig.17 at Z=3 for k-ε model there is development of negative pressure. All pressure profiles are coincides between X=2.5m to X=3m. Before coincides pressure is lower and after it is high. The contour plot corresponding to this pressure profile is in fig.18
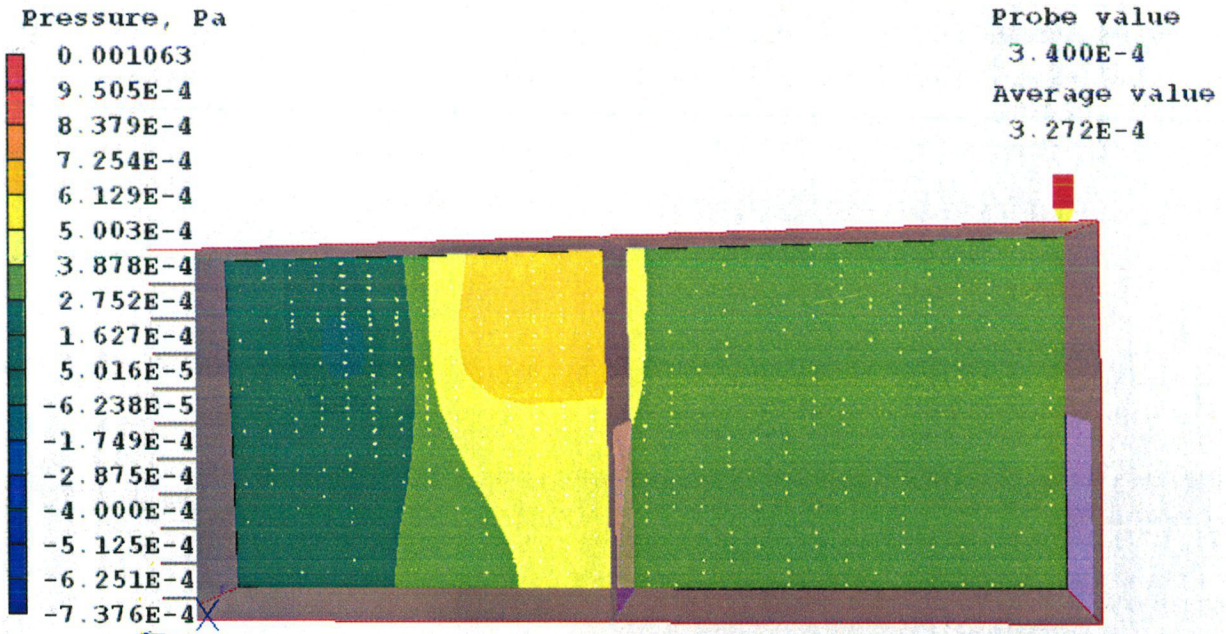
Fig.18 Contour plot of pressure at Y=2m
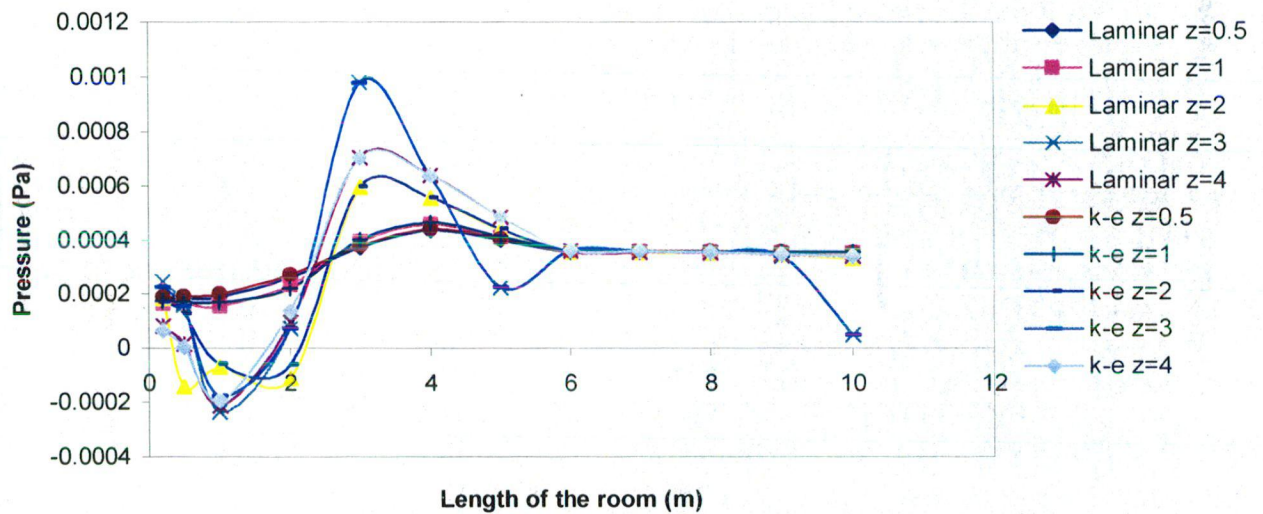
Fig.19 Pressure profile at Y=3m for different heights

From fig.19 there is development of negative pressure at the inlet and as length proceeds pressure is increasing and decreasing and becomes constant. The contour plot corresponding to this pressure profile is in fig.20

56
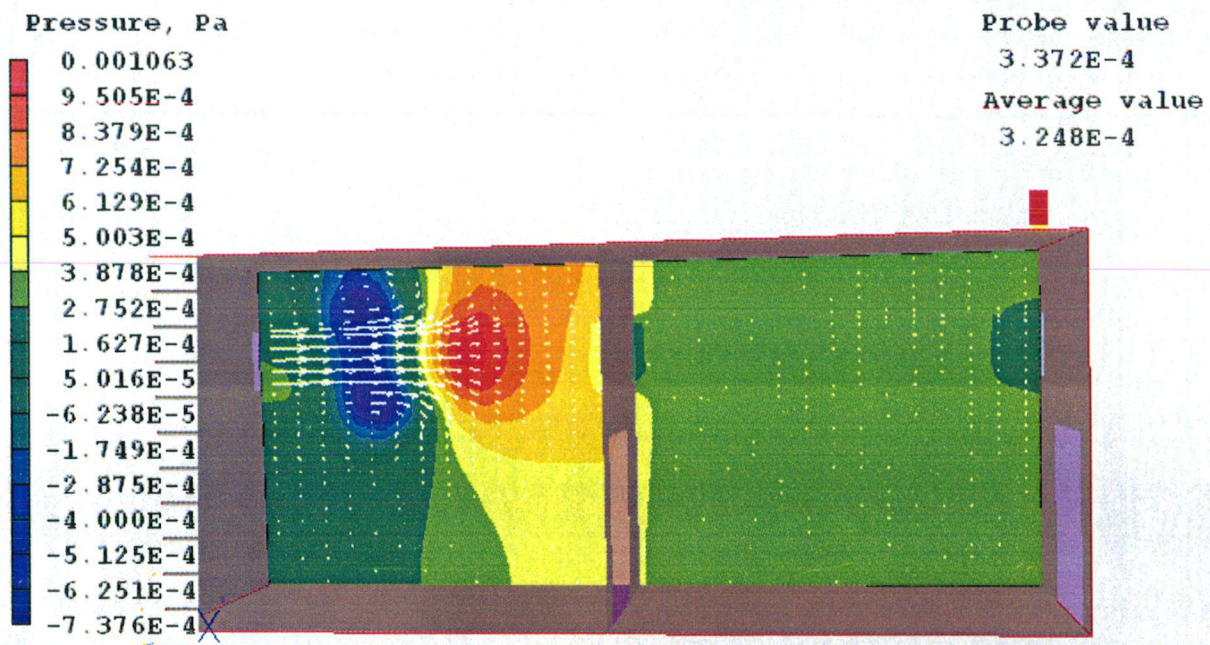
Fig.20 Contour plot of pressure at Y=3m
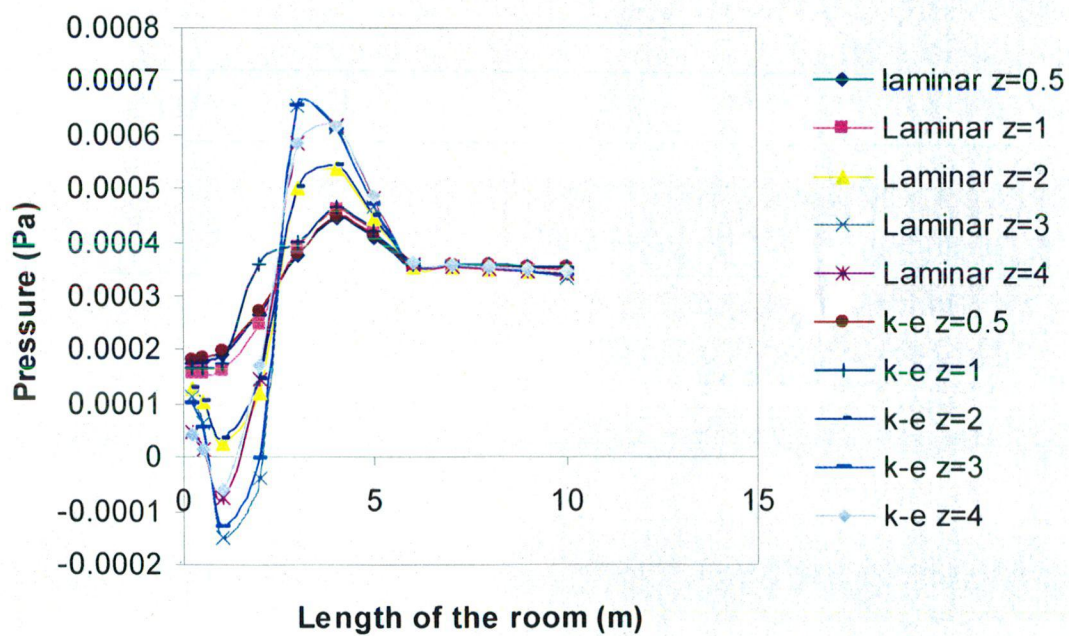
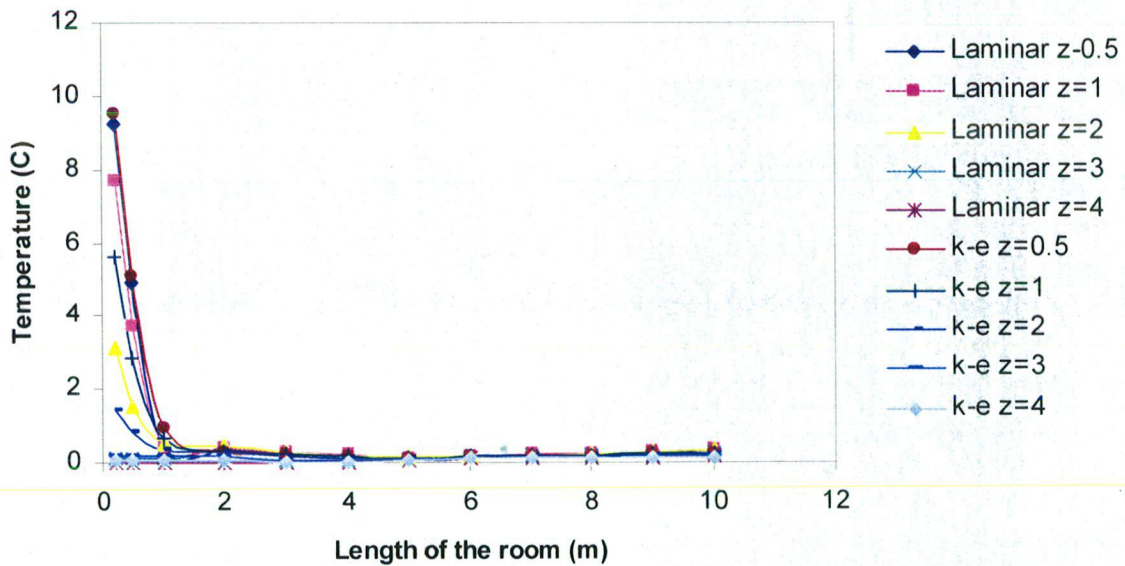Fig.21 Pressure profile at Y=4m for different heights

From fig.21 there is development of negative pressure at the inlet and as length proceeds pressure is increasing and decreasing and becomes constant. The contour plot corresponding to this pressure profile is in fig.22

57
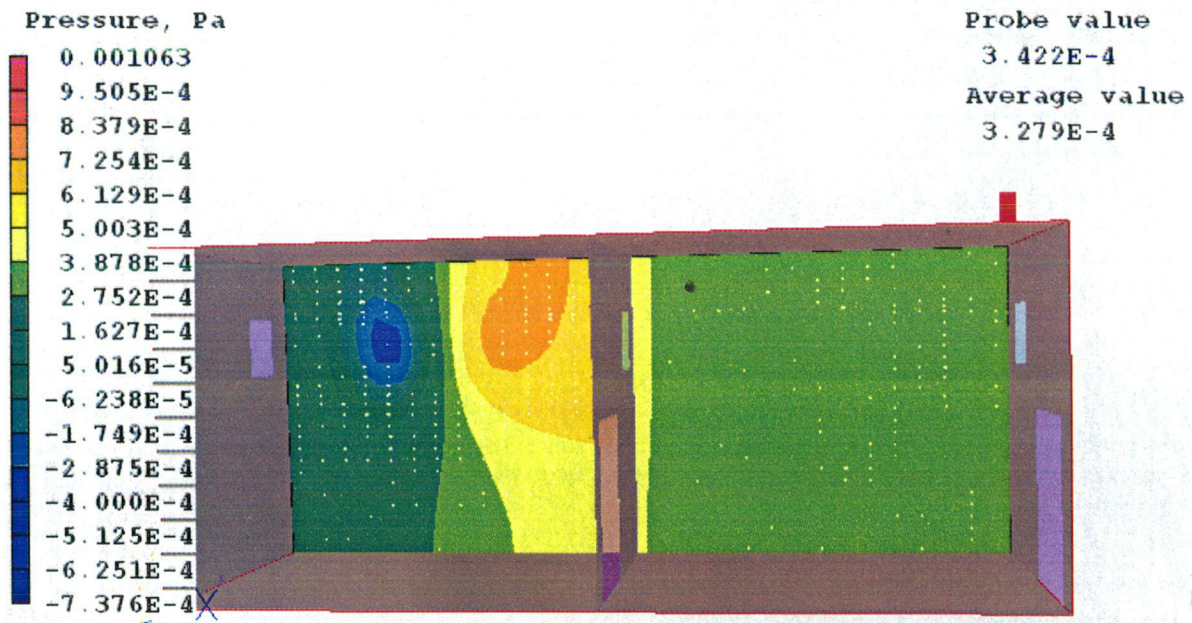
Fig.22 Contour plot of pressure at Y=4m
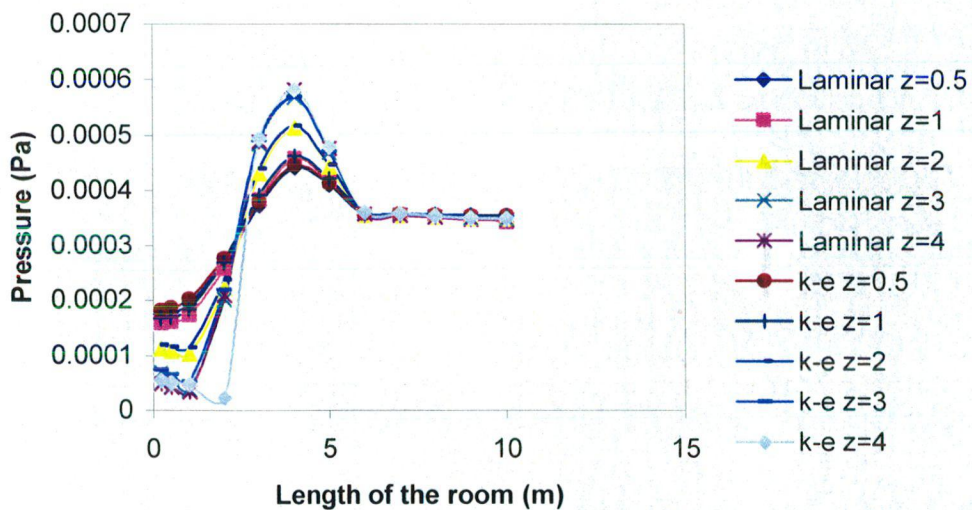
Fig.23 Pressure profile at Y=5m for different heights

From fig.23 there no negative pressure near to wall and the pressure fluctuate from low to high and become constant. The contour plot corresponding to this pressure profile is in fig.24

58
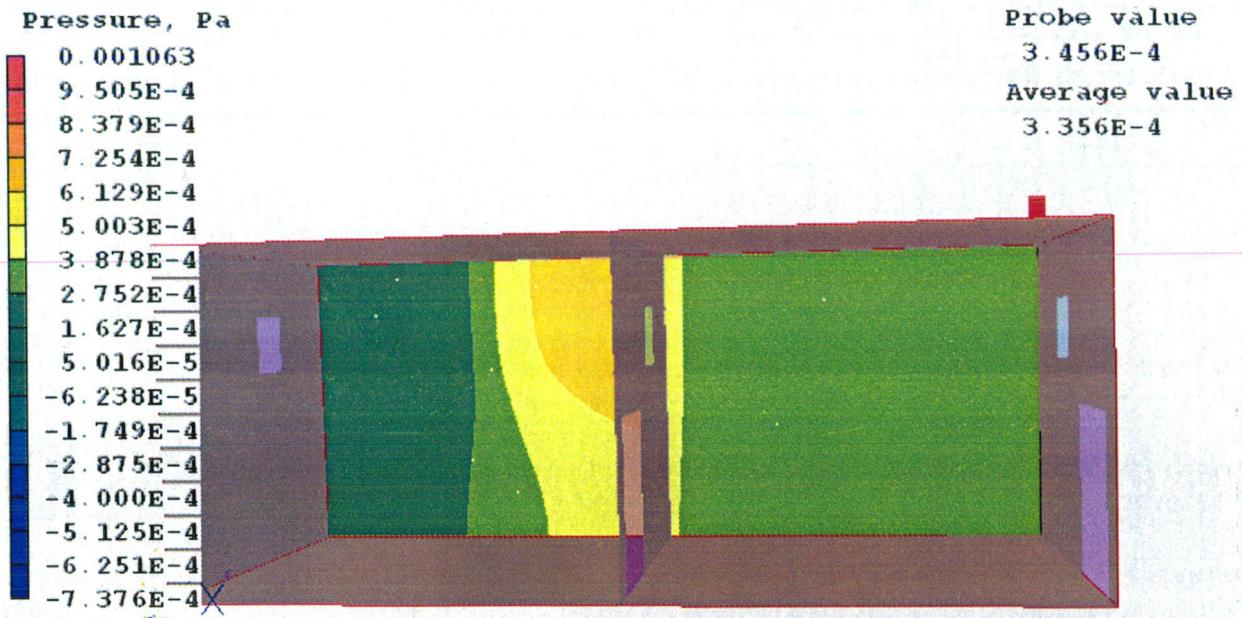
Fig.24 Contour plot of pressure at Y=5m

From pressure plots, as I have not given any input pressure there is development of negative pressure near to inlet which should not be the case. So for indoor air quality there should be room pressure have to be specified. The remaining part of the room, fluctuations in pressure is there till is enters to rest room.

6.2.3 Variation/Profiles of Temperature
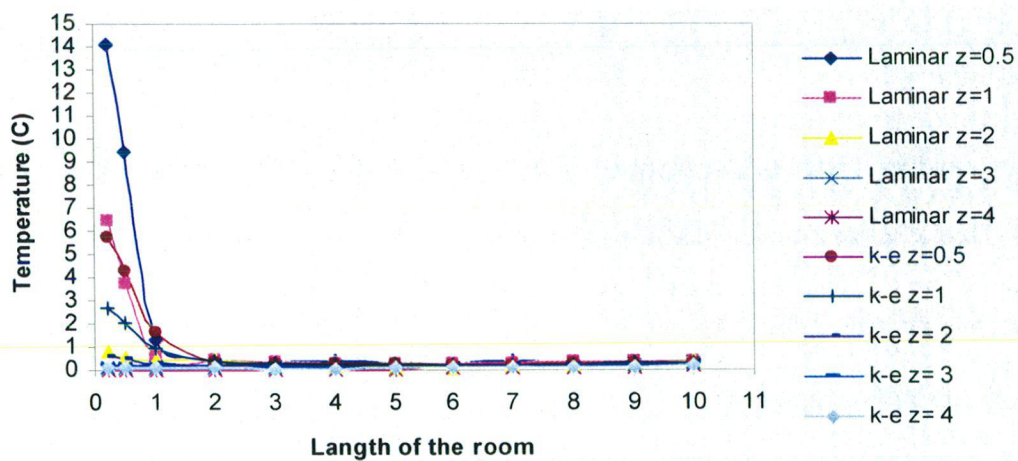
Fig.25 Temperature profile at Y=1m for different heights

59

From fig.25 at the corner of the room where contaminant enters with temperature, high temperature is present and as the length and width proceeds it becomes low and constant. The contour plot corresponding to this temperature profile is in fig.26
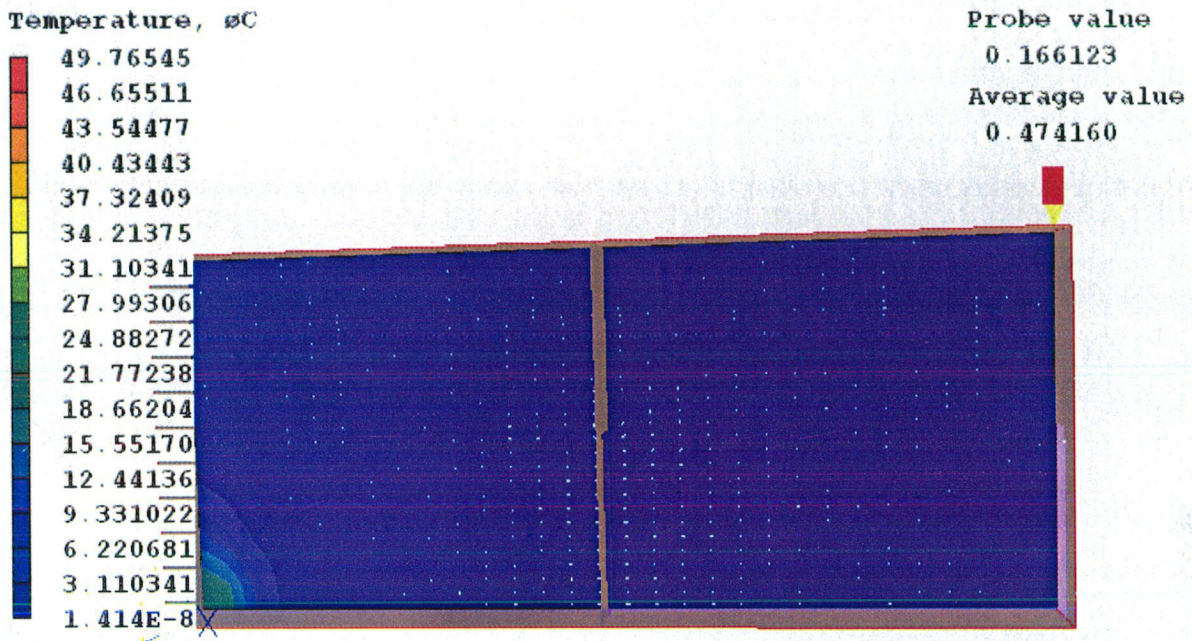

Fig.26 Contour plot of temperature at Y=1m

Fig.27 Temperature profile at Y=2m for different heights

From fig.27 at the corner of the room where contaminant enters with temperature, high temperature is present and as the length and width proceeds it becomes low and constant. The contour plot corresponding to this temperature profile is in fig.28.
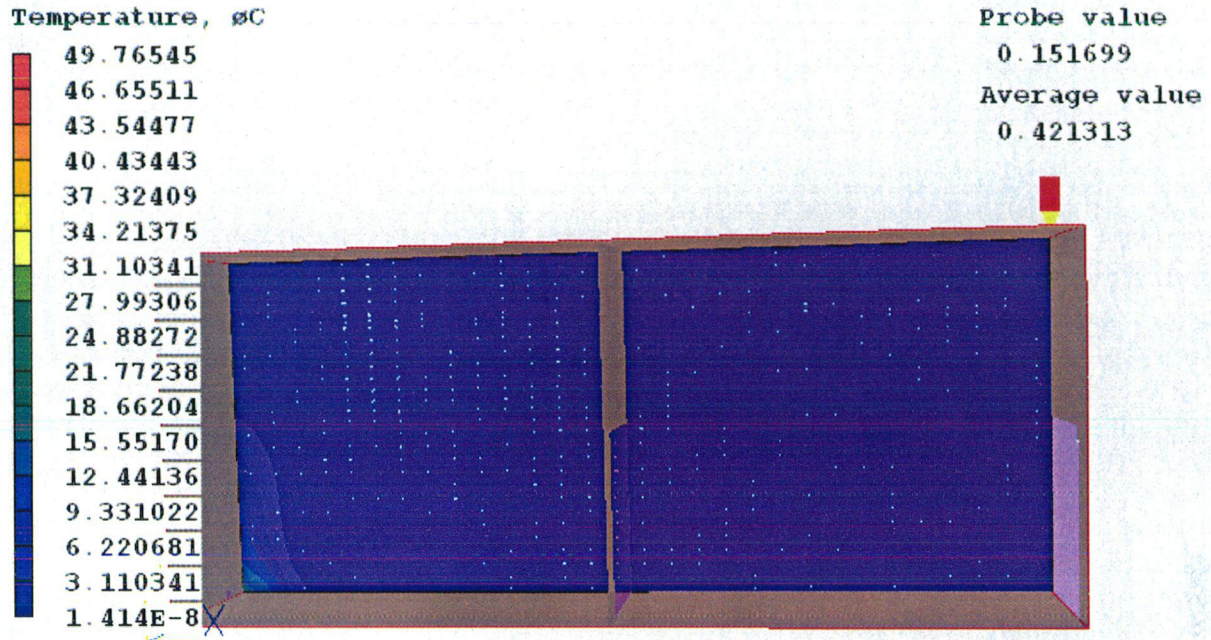
Fig.28 Contour plot of temperature at Y=2m
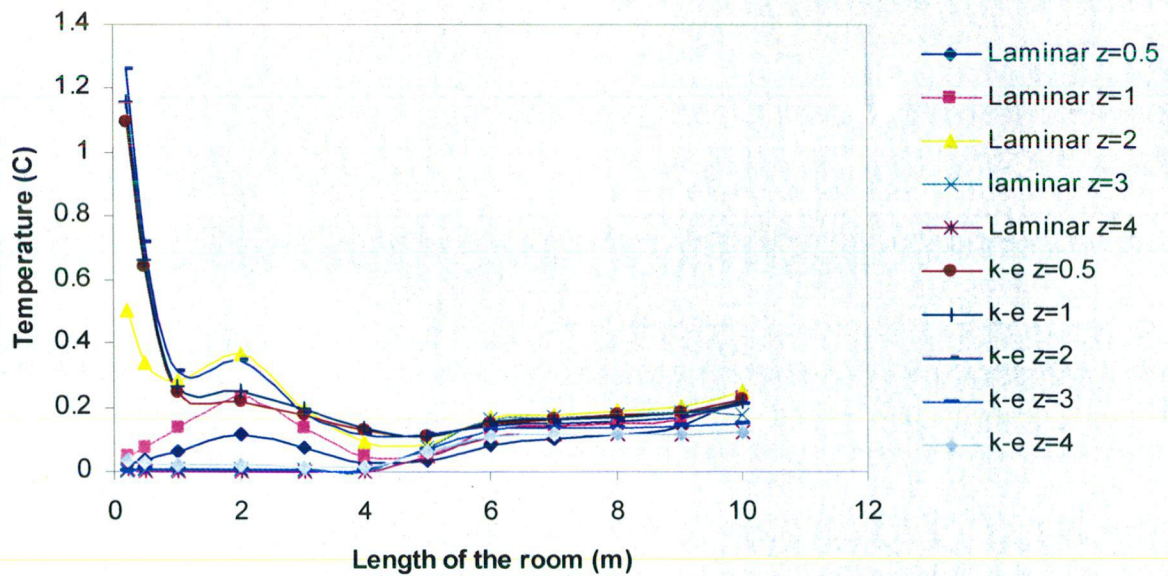
Fig.29 Temperature profile at Y=3m for different heights

From fig.29 at above the contaminant source temperature is high and as it proceeds through the length it becomes low. The contour plot corresponding to this temperature profile is in fig.30
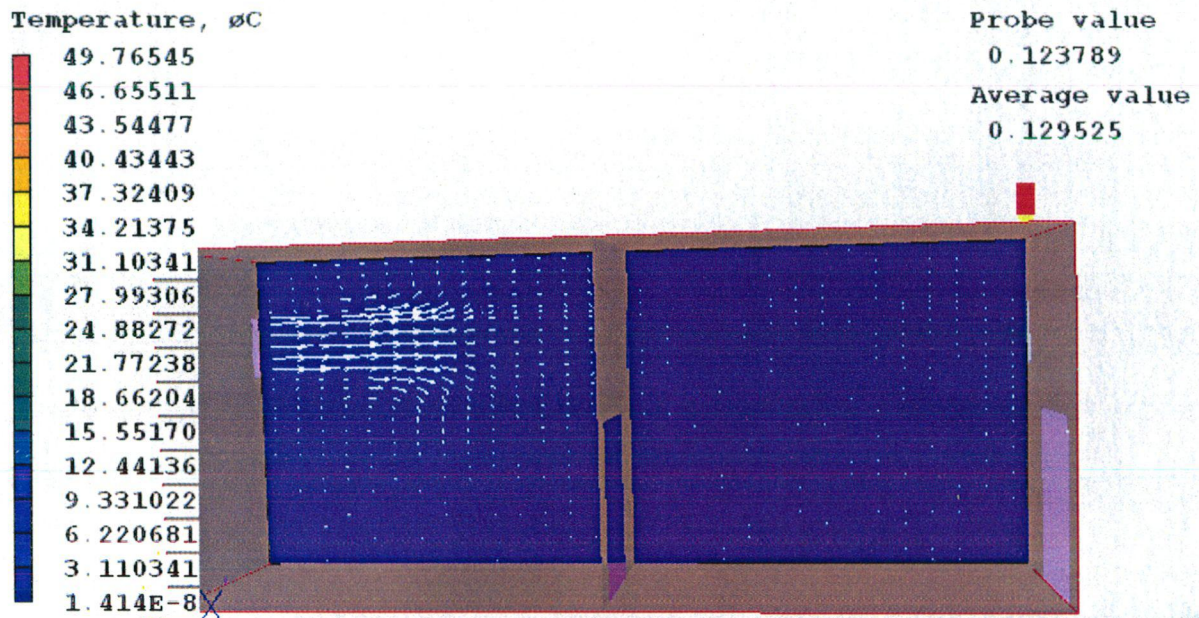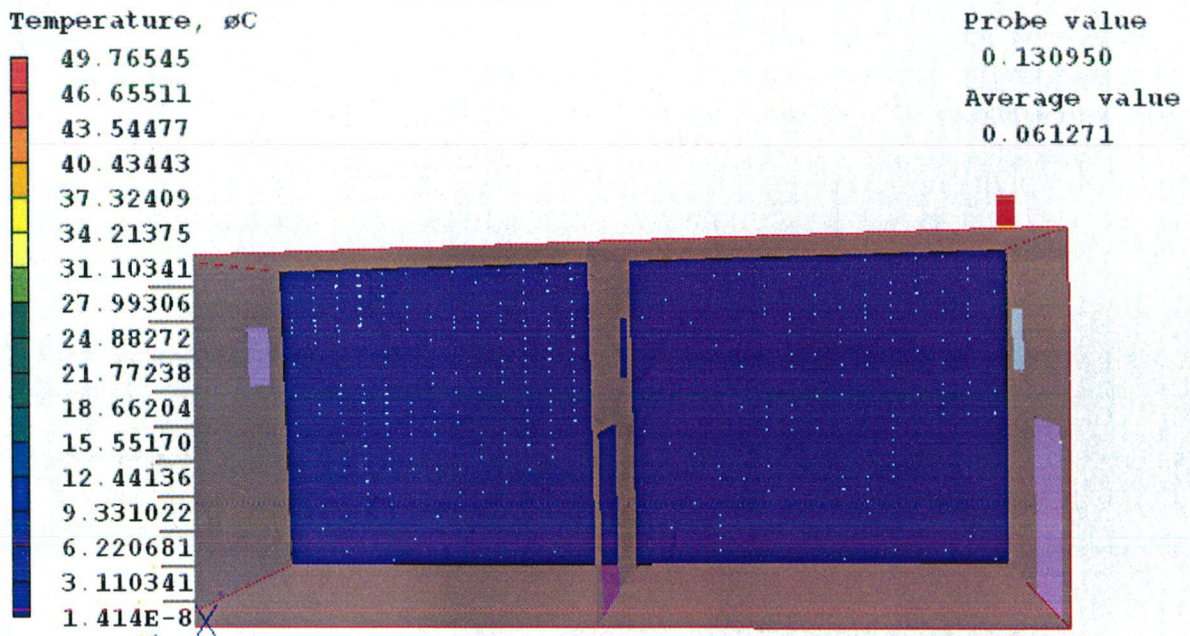

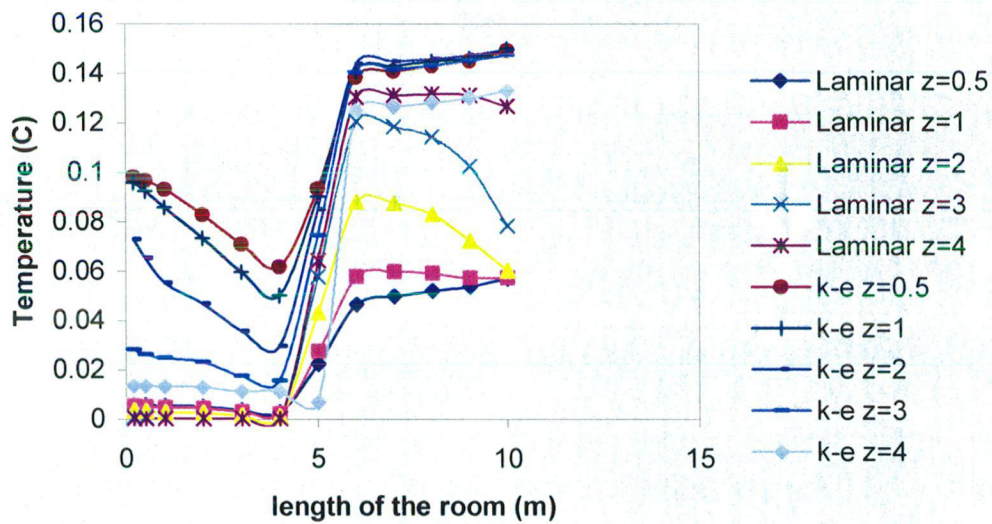Fig.30 Contour plot of temperature at Y=3m
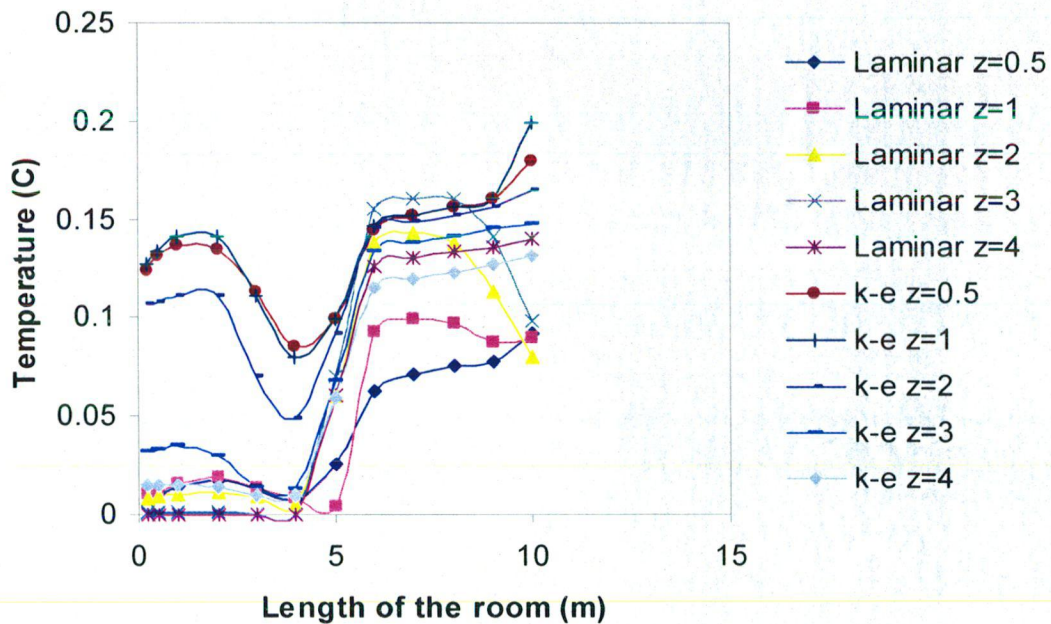
Fig.31 Temperature profile at Y=4m for different heights

From fig.31 as these profiles is near to ceiling temperature is high and it decreases slightly as it moves along the length. At beginning of the rest room

there is slight temperature increase. The contour plot corresponding to this temperature profile is in fig.32.
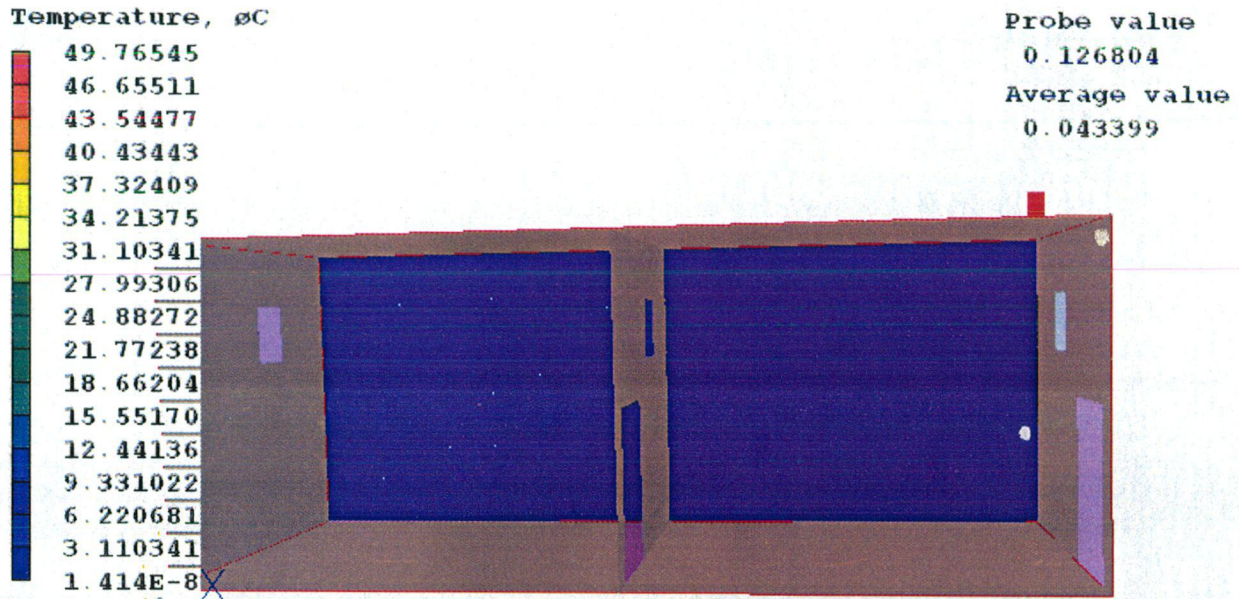

Fig.32 Contour plot of temperature at Y=4m

Fig.33 Temperature profile at Y=5m for different heights

From fig.33 as these profiles are at ceiling temperature is high and it decreases slightly as it moves along the length. At beginning of the rest room there is slight temperature increase. The contour plot corresponding to this temperature profile is in fig.34.

Fig.34 Contour plot of temperature at Y=5m

From temperature plots, it is clear that the temperature of contaminant is not affecting the process controls. As the contaminant enters the temperature is high at that point and as it reaches to normal after one meter. So there is no effect of temperature on process controls and on the rest room.
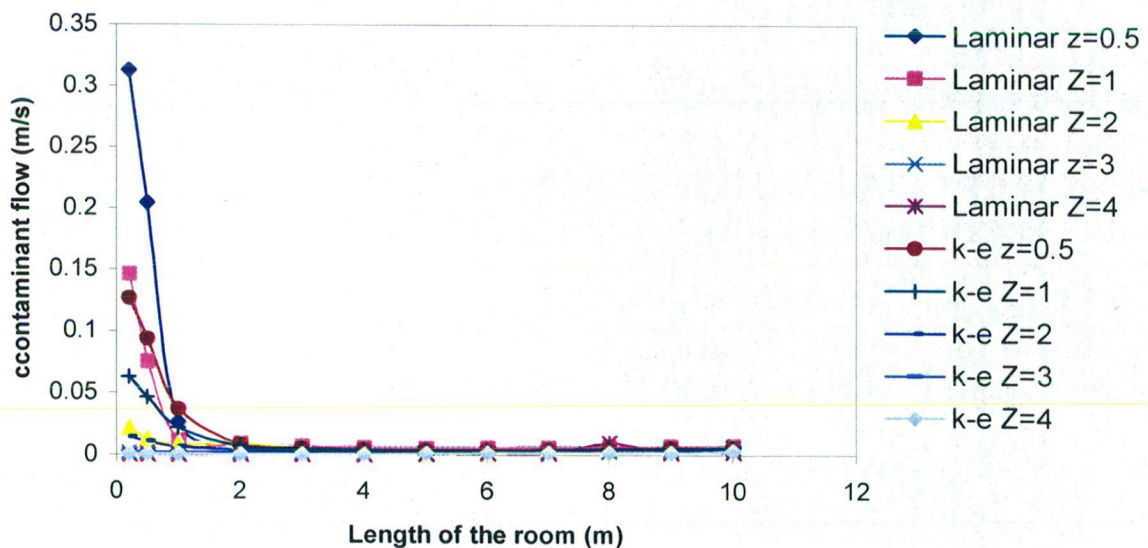
6.2.4 Variation/Profiles of Contaminant flow

Fig.35 Contaminant profile at Y=1m for different heights

From fig.35 as it is near to contaminant source there is high contaminant flow in the beginning and as the length proceeds flow becomes lower. The contour plot corresponding to this contaminant flow profile is in fig.36.
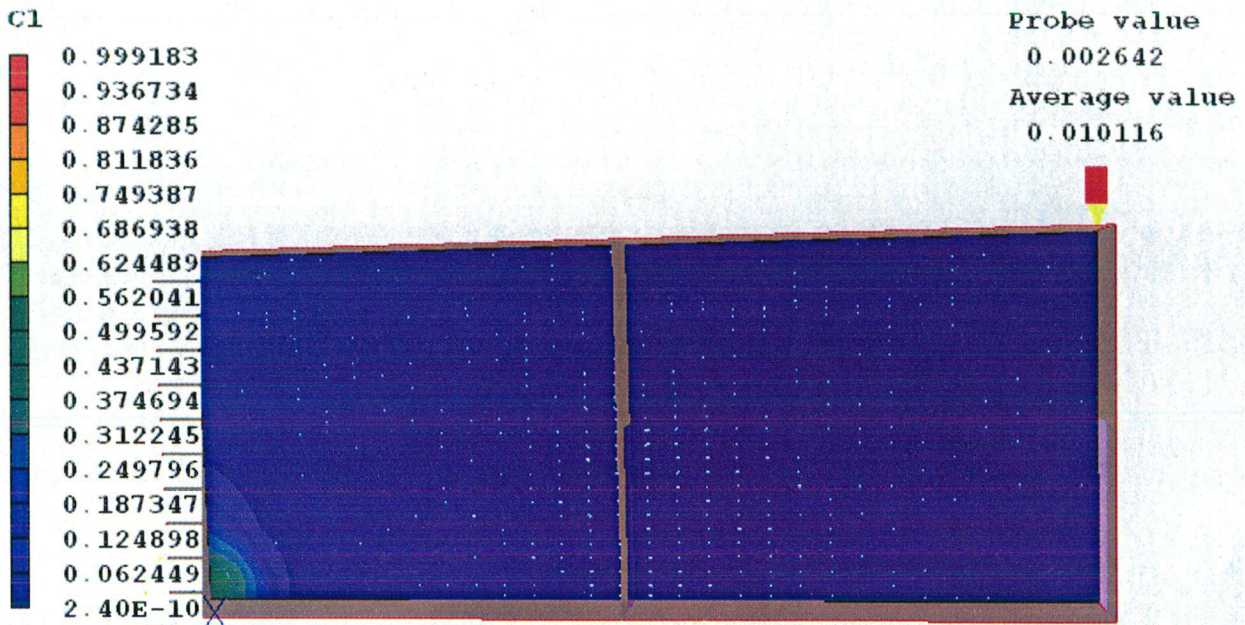

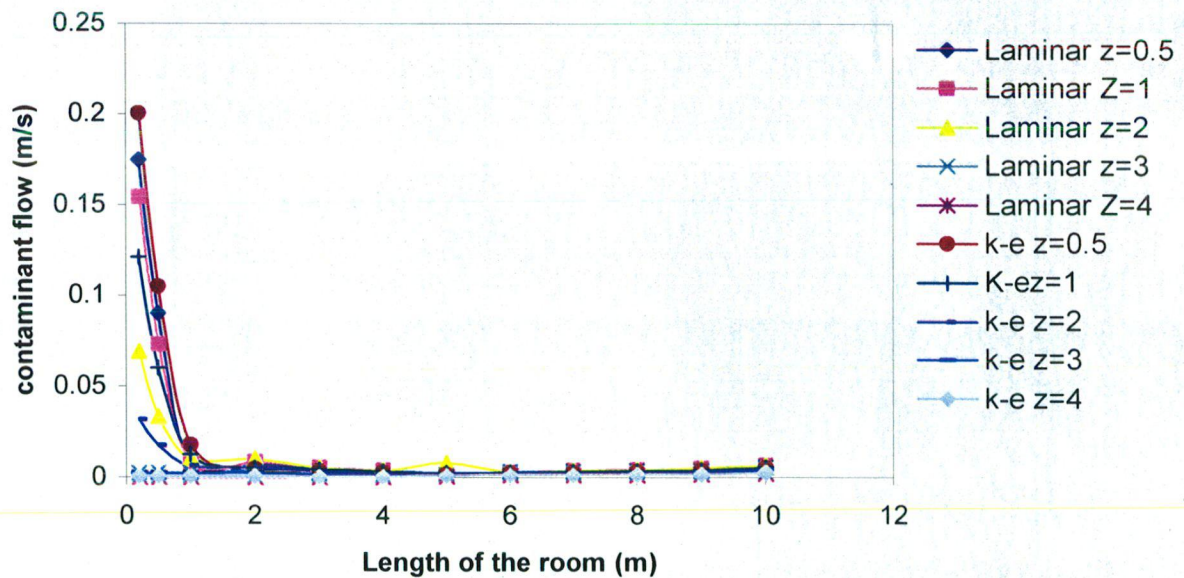Fig.36 Contour plot of contaminant at Y=1m

Fig.37 Contaminant profile at Y=2m for different heights

65

From fig.37 as it is near to contaminant source there is high contaminant flow in the beginning and as the length proceeds flow becomes lower. The contour plot corresponding to this contaminant flow profile is in fig.38.
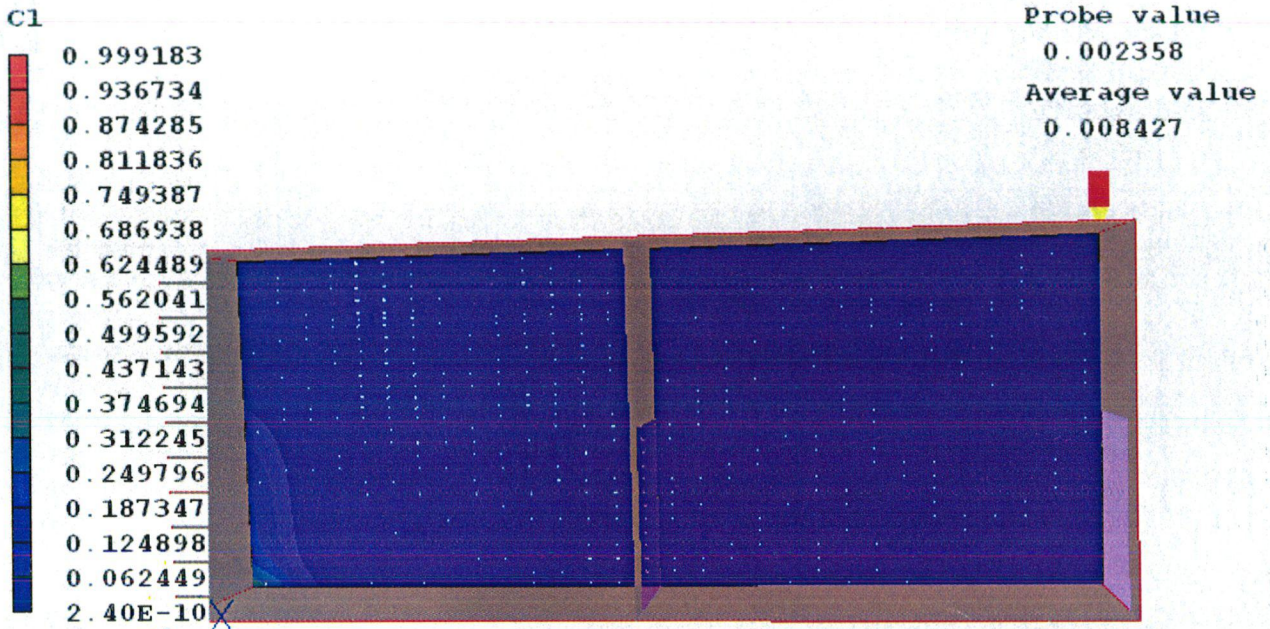

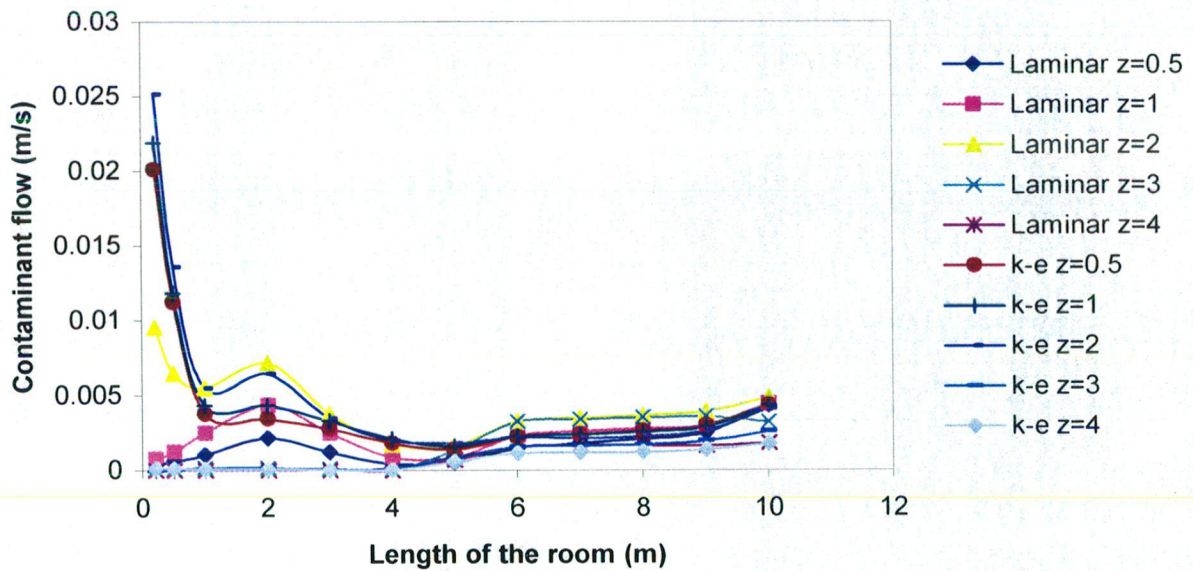Fig.38 Contour plot of contaminant at Y=2m

Fig.39 Contaminant profile at Y=3m for different heights

66

From fig.39 high contaminant flow in the beginning is present and as the length proceeds flow becomes lower. The contour plot corresponding to this contaminant flow profile is in fig.40.

C1

0.999183	
0.936734	
0.874285	
0.811836	
0.749387	
0.686938	
0.624489	
0.562041	
0.499592	
0.437143	
0.374694	
0.312245	
0.249796	
0.187347	
0.124898	
0.062449	
2.40E-10	

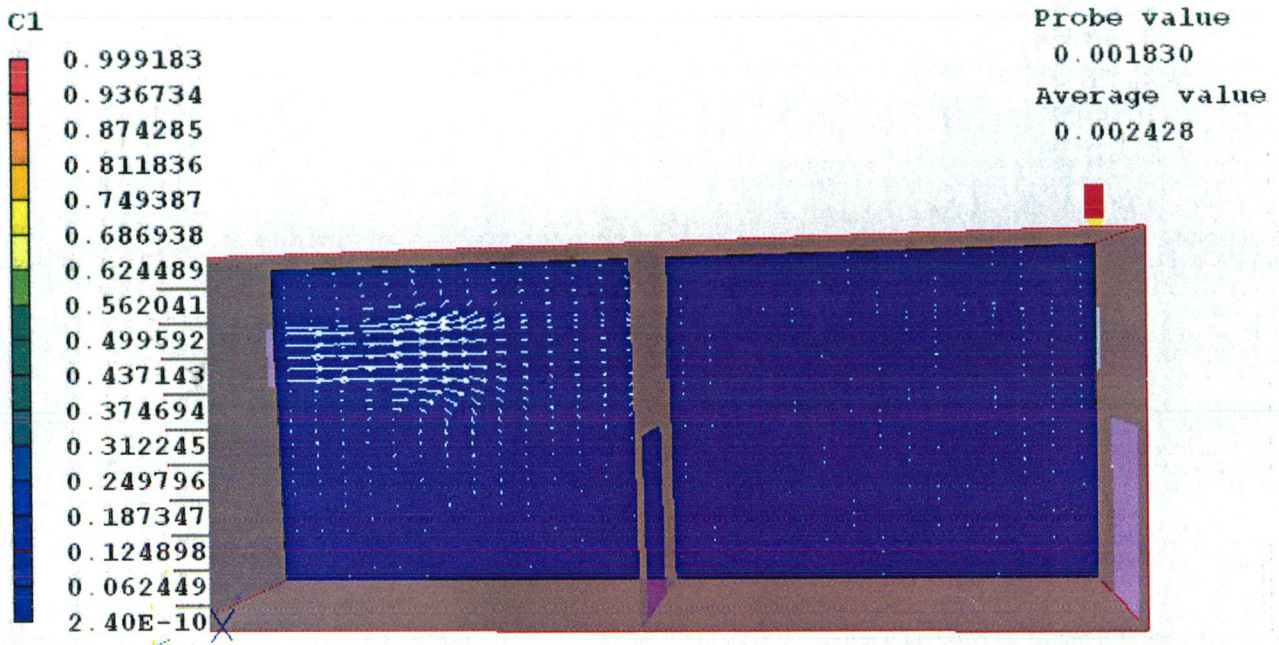Probe value
0.001830
Average value
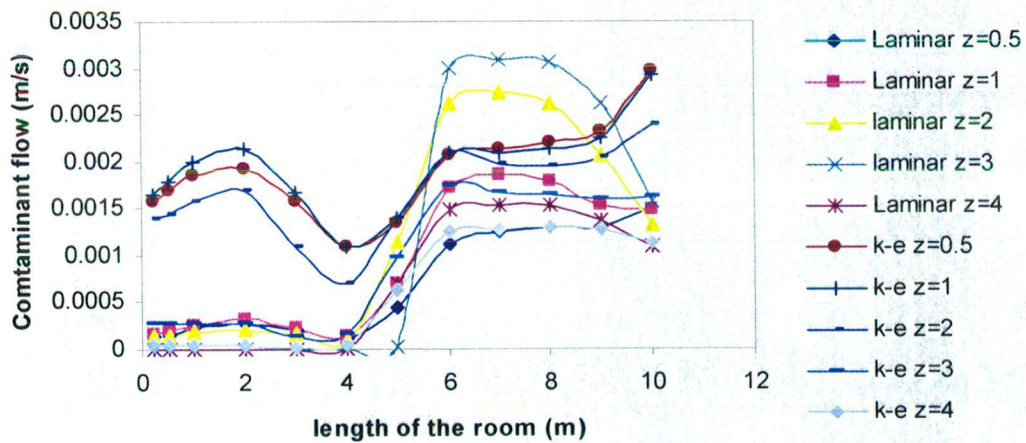0.002428

Fig.40 Contour plot of contaminant at Y=3m

Fig.41 Contaminant profile at Y=4m for different heights

From fig.41 there are contaminant fluctuations at the inlet due to negative pressure development. At the entrance of control panel room high contaminant is present due to presence of vectors at the wall. There is a drastic change at the wall. The contour plot corresponding to this contaminant flow profile is in fig.42.
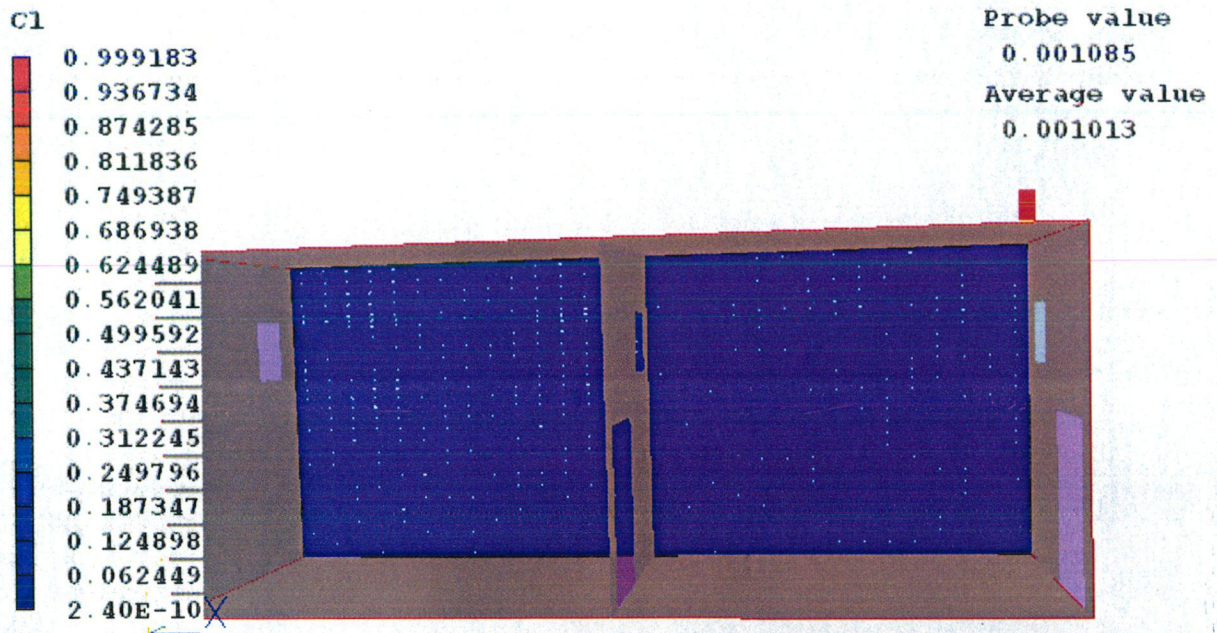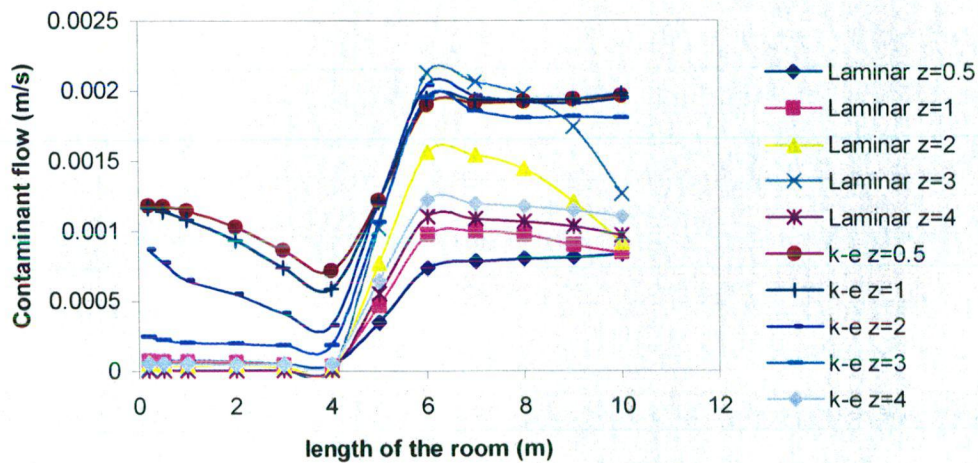
Fig.42 Contour plot of contaminant at Y=4m

Fig.43 Contaminant profile at Y=5m for different heights

From fig.43 there are contaminant fluctuations at the inlet due to negative pressure development. At the entrance of control panel room high contaminant is present due to presence of vectors at the wall. There is a drastic change at the wall. The contour plot corresponding to this contaminant flow profile is in fig.44

C1
0.999183
0.936734
0.874285
0.811836
0.749387
0.686938
0.624489
0.562041
0.499592
0.437143
0.374694
0.312245
0.249796
0.187347
0.124898
0.062449
2.40E-10

Probe value
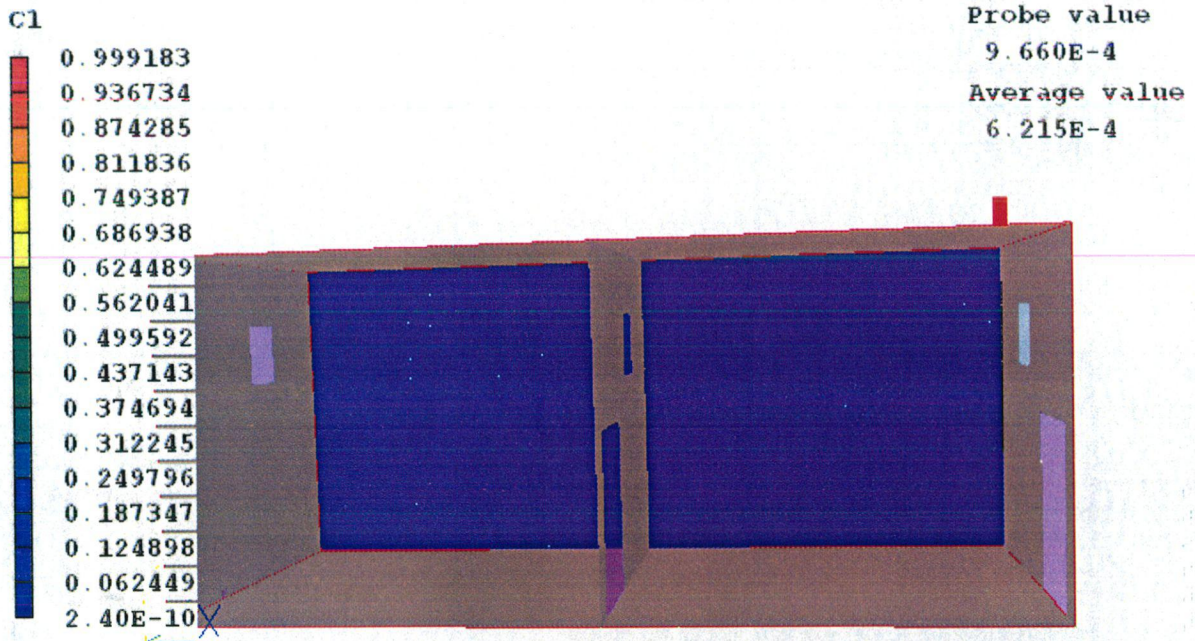9.660E-4
Average value
6.215E-4

Fig.44 Contour plot of contaminant at Y=5m

If the contaminant concentration is high, it will be a serious problem. But due to air inlet, there is dilution in contaminant and it is not affecting in control panel room. Also contaminant is not affecting the persons who are supposed to be in rest room.

6.3 Comparison of laminar and k-ε model:-
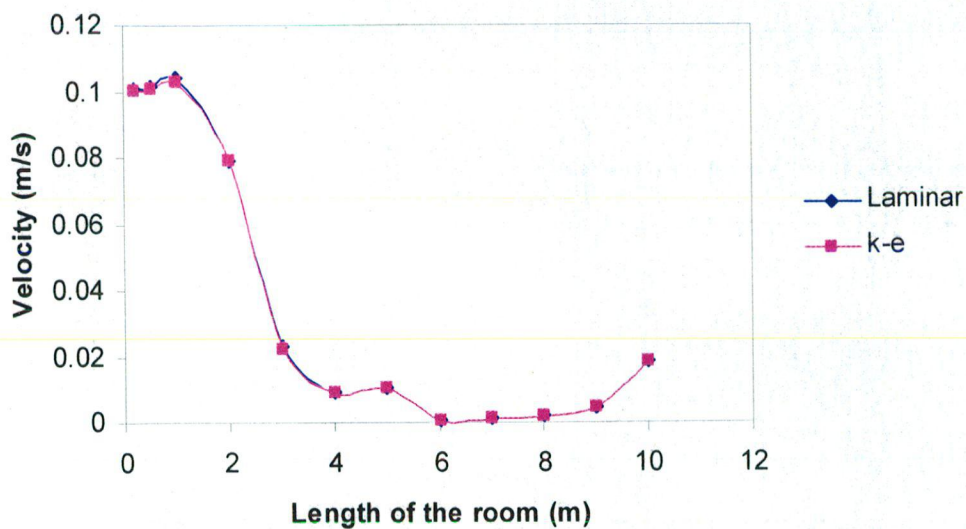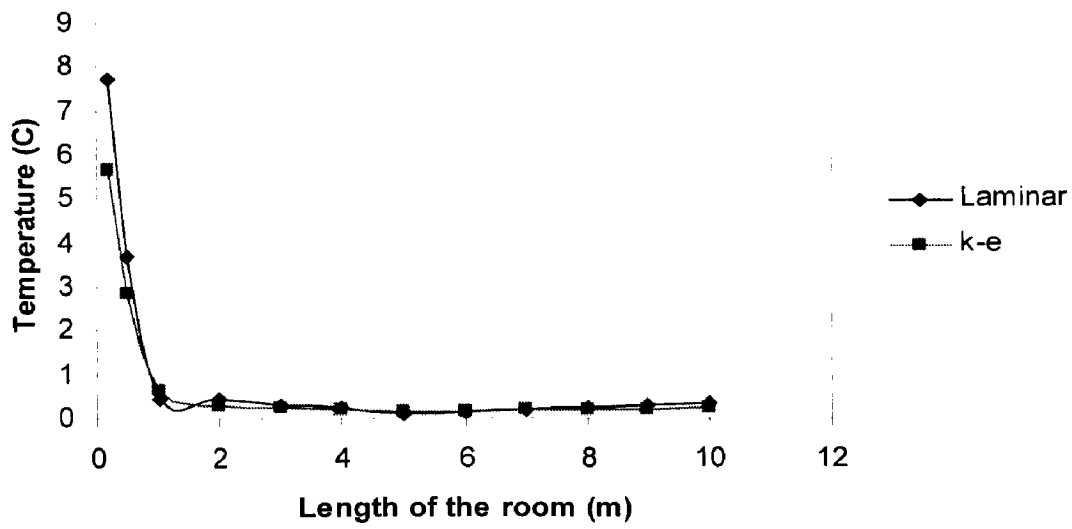

Fig.45 Velocity profile for laminar and k-ε model

69

Fig.46 Temperature profile for laminar and k-ε model
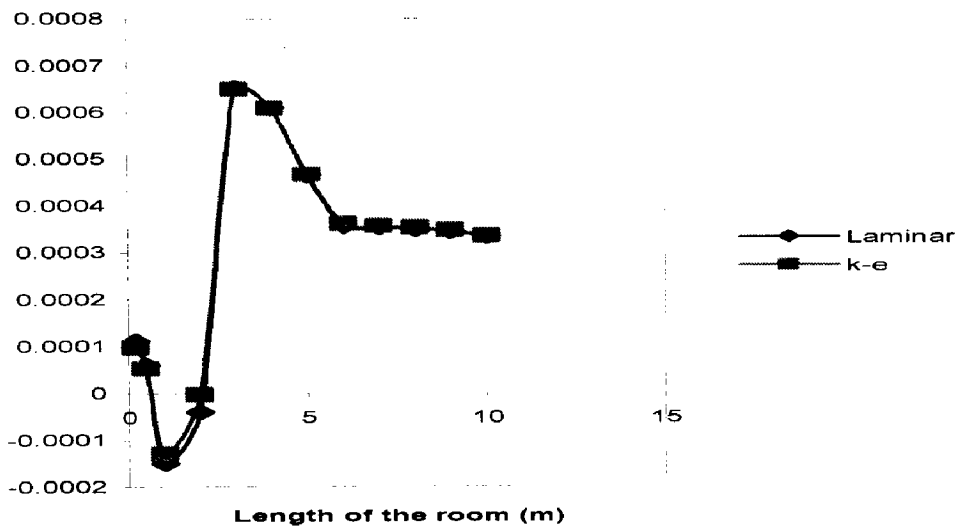

Fig.47 Pressure profile for laminar and k-ε model

70
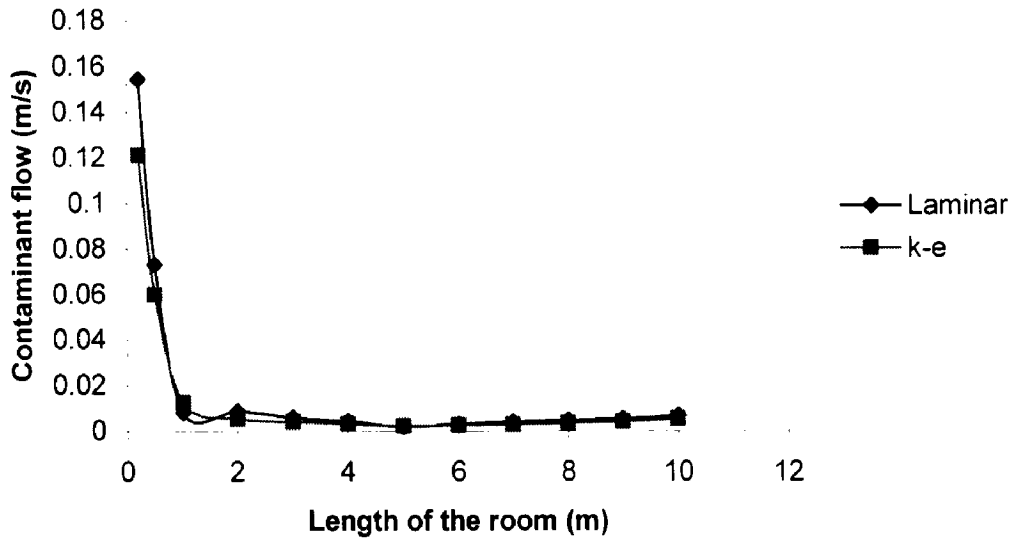
Fig.48 Contaminant flow profile for laminar and k-ε model

For simulating simple indoor air flows standard k-ε predicts actual flow patterns. k-ε model is based on the assumption of high Reynolds number flow. The standard k-ε model predicts velocities nearly close to the laminar model. For pressure k-ε model predicts slightly lower than the laminar models. For pressure and contaminant k-ε model is differs more in beginning and it slightly lower than laminar model. Therefore laminar model predicts good results than k-ε model.

Detailed measurements of indoor air flow are generally difficult to accomplish because, behaviors at the boundaries of rooms (including walls, partitions, and furniture) can have a large effect on flow motion. It is necessary, therefore, to resolve at fine scale the behaviour near surface and at the same time make measurements over the entire room space.

This work approaches this measurement by taking readings at different heights and widths with respect to length of the room. The flows are modeled with a standard CFD numerical code PHOENICS. Of the flow models examined, laminar model showed better than k- ε model.

Air velocity near the inlet is like a jet and is low in remaining part of the room is predicted accurately. Pressure fluctuations are high in control panel room and constant in rest room. There is no effect of temperature on process controller. No effect of contaminant on control panel and rest room.

Our flows are at low speeds, and the effects of turbulence do not significantly influence the basic flow patterns and velocities.

In this dissertation the velocity profiles, pressure profiles, temperature profiles and contaminant flow profiles are studied at steady state.

In future the work can be extended to unsteady state or transient state, so that up to how much time is required to reach high temperature near the process controllers to get damaged and also to people in rest room. How much time it requires for contaminant to effect on people in rest room.

In this thesis only one CFD package is used. Comparison can be done by taking simulation of same model in different packages like Fluent, CFX etc.

1. Boussineq, J., 1877: *"Theorie de lecoulement tourbillan"t*. Mem.pres. acad. Sci. (paris) XXIII , 46.

2. Brohus, H., 1997: *"Personal Exposure to Contaminant Sources in Ventilated Rooms"*, Engineering and Science, Aalborg University, PhD Thesis, 264 pp.

3. Cham, *"The main features of phoenics"*
(http://www.cham.co.uk/phoenics/d_polis/d_docs/tr001/tr001.htm#what)

4. Dannevik, W. P., Yakhot, V., and Orszag, S. A., 1987: *"Analytical theories of turbulence and the ε expantion"*. Phys. Fluids, vol.30, 2021.

5. Davidson, L., 2003: *"An Introduction to Turbulence Models"*. Department of Thermo and Fluid Dynamics, Chalmers University of Technology, Göteborg.

6. Eisenga. A. H. M., Cyclone fluid dynamics: *"application of CFD in the industry, CFD for process-technology flow problems"*
(http://www.cyclone.nl/main/application_of_CFD.htm)

7. Einberg Gery, June 2005: *"Air diffusion and solid contaminant behaviour in room ventilation-a CFD based integrated approach"*, KTH industrial engineering and management, doctorial thesis.

8. Fanger, P. O., 1970: *"Thermal comfort"*, Technical University of Denmark.

9. Fanger, P. O., Melikov, A. K., Hanzawa, H., and Ring, J., 1988: *"Air Turbulence and Sensation of Draught"*. Energy and Buildings, vol.12, pp.21-39.

10. FLUENT Inc, 2003: *"FLUENT 6.1 User's Guide"*, Digital Copy.

11. Forster, D., Nelson, D., and Stephen, M., 1977: *"Large-distace and long time properties of a randomly stirred fluide"*. Phys.rev.A vol.16, 732 and 1976: *"Longtime tails and the large-eddy behaviour of a randomly stirred fluide"*. Phys.rev.lett. vol.36, 867.

12. Health Canada, "Environmental and workplace health". (http://www.hc-sc.gc.ca/ewh-semt/index_e.html).

13. Hinze, J.O. 1987: *"Turbulence (2nd edition)"*. McGraw-hill. New York.

14. Jones, W.P., and Launder, B.E., 18th September 1972: *"The calculation of low-reynolds-number phenomena with a two equation model of turbulence"*. International journal of heat and mass transfer. Vol.16, pp.1119-1130.

15. Jones, A. P., 1999: Indoor air quality and health. *"Atmospheric Environment"*, vol.33, 4535-4564.

16. Kakumanu, R., June 2006: "Study of air flow in a room with and without wall temperature differentials", IITR, M.tech Thesis.

17. Krühne, 1995: Energy- and Mass Transfer in Rooms with Displacement Ventilation. *"Proceedings of Healthy Buildings '95, Fourth International Conference on Healthy Buildings"*, Milan, Italy, 11-14 September

18. Lam, S. H., 23rd January 1992 : *"On the RNG theory of turbulence"*. physics of fluids A, vol.4, no.5

19. Launder, B. E., and Spalding, D. B., 1974: *"The numerical computation of turbulent flow"*. Comput. Methods Mech. Eng., 3, 269-289.

19. Launder. B. E. and D. B. Spalding, 1974: *"The numerical computation of turbulent flows"*, Comput. Meth. Appl Mech. Eng., 3 269 - 289.

20. Layers., 1967: Morgan Grampian, London.

21. Luo, S., 2003: *"Numerical Study of Three Dimensional Turbulent Flows in a Habitat With Coupled Heat and Mass Transfer"*, Mechanics, University of the Mediterranean (University of Aix-Marseille II).

22. Matson, U., 2004: *"Ultrafine particles in indoor air - measurements and modelling"*, Building Services Engineering, Chalmers University of Technology, PhD thesis, Göteborg, 76 pp.

23. Mundt, E., 1996: *"The Performance of Displacement Ventilation Systems - Experimental and Theoretical Studies"*, Building Services Engineering, KTH (Royal Institute of Technology, Stockholm, Ph.D thesis, 155 pp.

24. Patankar, S. V., and Spalding, D. B., 1980: *"Heat and mass transfer in boundary"*.

25. 5. Qingyang, C., 1986: *"The Mathematical Foundation of the CHAMPION SGE Computer Code"*, Report No. K-118, Delft University of Technology.

26. Qingyan, C., van der Kool, J., and Meyers, AT., 11th February 1988: *"Measurement and Computations of ventilation efficiency and temperature efficiency in a ventilated room"*. Energy and building, vol.12 pp. 85-99

27. Rosten, H. I., and Spalding, D. B., 1981: *"The Mathematical Basis of the PHOENICS EARTH Computer Code"*, Report TR/58b, CHAM Ltd., London.

28. Spalding, B., 13th April 1999; *"EUROTEX workshop on internet and web-based computing"*.

29. The inside story, *"A guide to indoor air quality"*. CPSC document # 450. (http://www.cpsc.gov/the%20Inside%20Story%20A%20Guide%20to%20Indoor%20Air%20Quality.htm)

30. Versteeg, H. K., and Malalasekera, W., 1995: *"An Introduction to Computational Fluid Dynamics - The Finite Volume Method"*. Prentice Hall, London, 272 pp.

31. Yakhot, V., and Orszag, S. A., 1986: *"Renormalization group analysis of turbulence I". basic theory.* Journal of science computing, vol.3.

32. Youchen, F., 1995: *" CFD modelling of the air and contaminant distribution in rooms"* Energy and building, Vol.23 pp.33-39.